



# Lawrence Berkeley Laboratory

UNIVERSITY OF CALIFORNIA

## ENERGY & ENVIRONMENT DIVISION

RECEIVED  
LAWRENCE  
BERKELEY LABORATORY  
APR 16 1981  
LIBRARY AND  
DOCUMENTS SECTION

CATALYTIC OXIDATION OF S(IV) ON ACTIVATED  
CARBON IN AQUEOUS SUSPENSION: KINETICS  
AND MECHANISM

Richard Brodzinsky  
(Ph.D. thesis)

February 1981

### TWO-WEEK LOAN COPY

*This is a Library Circulating Copy  
which may be borrowed for two weeks.  
For a personal retention copy, call  
Tech. Info. Division, Ext. 6782*



LBL-12218  
c2

## DISCLAIMER

This document was prepared as an account of work sponsored by the United States Government. While this document is believed to contain correct information, neither the United States Government nor any agency thereof, nor the Regents of the University of California, nor any of their employees, makes any warranty, express or implied, or assumes any legal responsibility for the accuracy, completeness, or usefulness of any information, apparatus, product, or process disclosed, or represents that its use would not infringe privately owned rights. Reference herein to any specific commercial product, process, or service by its trade name, trademark, manufacturer, or otherwise, does not necessarily constitute or imply its endorsement, recommendation, or favoring by the United States Government or any agency thereof, or the Regents of the University of California. The views and opinions of authors expressed herein do not necessarily state or reflect those of the United States Government or any agency thereof or the Regents of the University of California.

LBL-12218

CATALYTIC OXIDATION OF S(IV) ON ACTIVATED  
CARBON IN AQUEOUS SUSPENSION:  
KINETICS AND MECHANISM\*

Richard Brodzinsky

Department of Chemistry  
Lawrence Berkeley Laboratory  
University of California  
Berkeley, California 94720

---

\* This work was supported by the Assistant Secretary for the Environment, Office of Health and Environmental Research, Pollutant Characterization and Safety Research, Division of the U.S. Department of Energy under Contract No. W-7405-ENG-48 and the National Science Foundation.



Catalytic Oxidation of S(IV) on Activated  
Carbon in Aqueous Suspension:  
Kinetics and Mechanism\*

Richard Brodzinsky

Abstract

Activated carbon and combustion produced soot particles have been studied for their catalytic effect on the oxidation of aqueous sulfur(IV) species. These particles are found to be effective catalysts for the reaction. Detailed kinetic studies of the reaction were performed on three different activated carbons and on a soot collected in a highway tunnel. Combustion produced soots were tested for their catalytic behavior and found to be similar to the activated carbons.

The reaction rate was found to be linearly dependent on the concentration of carbon particles in the solution. The rate was found to follow a Langmuir adsorption isotherm for its dependence on oxygen and the product of two adsorption isotherms for S(IV).

The reaction is independent of the pH of the solution when the pH is below 7.6. The reaction does not occur when the pH is above 7.6. The three aqueous S(IV) species are catalyzed in their oxidation by

---

\* This dissertation has been published in part as: R. Brodzinsky, S. G. Chang, S. S. Markowitz, and T. Novakov, J. Phys. Chem., (1980) 84, 3354-3358.

the carbon particles in a similar manner. The pH cut-off is suggested as being a function of the catalytically active sites on the carbon surface. Activation energies for the reactions on the different carbons are all about 8.5 kcal/mole.

A possible four-step reaction mechanism is proposed. It consists of the adsorption of a dissolved oxygen molecule onto the carbon surface, followed by the adsorption of two S(IV) molecules or ions. These are oxidized on the surface to sulfate, which desorbs from the surface, regenerating the catalytically active site.

## CONTENTS

I.	INTRODUCTION . . . . .	1
	A. Air pollution. . . . .	1
	B. Atmospheric Sulfur . . . . .	3
	C. SO <sub>2</sub> Oxidation Mechanisms . . . . .	4
	D. Carbonaceous Particles as a Pollutant. . . . .	5
	E. Activated Carbon . . . . .	8
	F. Soot as an SO <sub>2</sub> Oxidation Catalyst. . . . .	8
	G. Objective. . . . .	9
	H. Note on Nomenclature . . . . .	11
II.	EXPERIMENTAL . . . . .	12
	A. Basic Setup. . . . .	12
	B. Preparation of Carbon Suspensions. . . . .	12
	C. Iodometric Determination of S(IV). . . . .	16
	D. Turbidimetric Determination of Sulfate . . . . .	18
	E. Ion Chromatography . . . . .	19
	F. Miscellaneous Techniques . . . . .	22
III.	RESULTS. . . . .	24
	A. Activated Carbons: Reaction and S(IV) Dependence . . . . .	24
	B. Oxygen and Temperature Studies . . . . .	34
	C. Combustion-Soot Studies. . . . .	41
	D. pH Effects . . . . .	41
	E. Other Studies. . . . .	48
IV.	DISCUSSION . . . . .	49
	A. Mechanism. . . . .	49
	B. Effects of pH. . . . .	56
	C. Confirmation of Results. . . . .	62
V.	SUMMARY AND CONCLUSIONS. . . . .	63
	ACKNOWLEDGEMENTS. . . . .	65
	APPENDIX A: Sample Data	
	1. Titration and Turbidity Data . . . . .	66
	2. IC Data. . . . .	67

APPENDIX B: Error Analysis and Computational Methods . . . . .	69
APPENDIX C: Abstract of "Kinetics and Mechanism for the Catalytic Oxidation of Sulfur Dioxide on Carbon in Aqueous Suspensions," J. Phys. Chem., 1980, <u>84</u> , 3354-3358. . . . .	74
REFERENCES AND FOOTNOTES. . . . .	75

## I. INTRODUCTION

### A. Air Pollution

The study of air pollution has only been of major interest to the scientific community since the end of World War II. The problem, though, has been around much longer. By his use of fire, man has always added pollutants into the atmosphere. It is hard to consider early man as a major source of pollution, but even before the Spanish settlement of California, the peculiar meteorology of the Los Angeles basin led the coastal Indians to name the place the "Valley of the Smokes." Nature also adds pollutants into the atmosphere.

As technology increased, so did man's energy requirements. Fossil fuels, in the form of coal and, in more recent historical times, oil, have come to be the major source of energy. Since the eighteenth century, use of these fuels has risen exponentially and the pollution has grown from the smokes of wood fires to the major urban problems which we are faced with today.

The earliest perceived problems were those related to the incomplete combustion of coal. Soot and ash abounded in the major industrial cities of the United States and Great Britain in the early twentieth century. Stories are told of the black films which would form on window sills and of how clean laundry could not be hung out to dry. But this problem was soon abated as newer, more efficient burning techniques were introduced, along with the first controls on the permissible emissions. By today's standards, these controls were crude and unscientific, but they served to reduce the soot problem to a point where the importance of soot as a pollutant was ignored until the 1970's.

As is so often the case, tragedy was needed to prompt the modern studies and control of air pollution. An air pollution episode killed twenty people in Donora, Pennsylvania in 1948, and over 4000 were killed in a London episode in 1952. The Los Angeles basin, after its growth during the war, became an area where visibility impairment is the norm. Months can go by without the San Gabriel Mountains being visible, and, especially during the 1950's and 60's, respiratory and eye irritation problems were at alarmingly high levels. It was there that a new word, "smog," was coined, being a combination of smoke and fog.

It was also in the Los Angeles area that the first modern studies of air pollution were performed. Haagen-Smit and coworkers at the California Institute of Technology in Pasadena were able to show that LA smog could be reproduced by the photochemical reactions of gaseous hydrocarbons and the oxides of nitrogen. It was these studies of "photochemical smog" which set the standards of research and control strategies for the following 25 years.

Air pollutants are divided into two general categories:

- 1) Primary - those emitted directly into the atmosphere, and
- 2) Secondary - those formed by subsequent reactions of primary pollutants. The first category includes soot, carbon dioxide, carbon monoxide, sulfur oxides, nitrogen oxides and hydrocarbons. The latter includes sulfuric and nitric acids, ozone and oxygenated organic compounds. It is the intent of this research to study how two primary pollutants, soot and sulfur dioxide, interact to form sulfuric acid.

## B. Atmospheric Sulfur

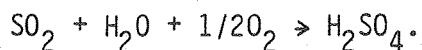
Sulfur as a pollutant exists mainly in three forms, reduced as hydrogen sulfide ( $\text{H}_2\text{S}$ ) and oxidized as sulfur dioxide ( $\text{SO}_2$ ) and sulfur trioxide ( $\text{SO}_3$ ). The two oxidized forms, which are species of the oxidation states S(IV) and S(VI), also exist as ionic species; bisulfite ( $\text{HSO}_3^-$ ), sulfite ( $\text{SO}_3^{2-}$ ), bisulfate ( $\text{HSO}_4^-$ ) and sulfate ( $\text{SO}_4^{2-}$ ). These sulfur containing species have many sources. They can come from man's burning of fossil fuels as well as from the decomposition and combustion of organic materials, sea salts and volcanoes. Man has little, if any, control over these natural sources of pollutant sulfur, which can contribute as much as 50 percent of the globally-emitted sulfur each year [1]. It is the remaining 50+percent which is of major interest in the development of air pollution control strategies. While nature's contribution is fairly uniformly spread around the globe (except in the case of volcanic eruptions), man concentrates his pollution around the areas in which he lives, but these pollutants can also be transported around the globe by winds.

The sulfur oxides contribute to the formation of acid rain and directly to deleterious health effects. Respiratory and cardiopulmonary problems have been shown to be caused by sulfur oxides (in particular sulfur dioxide) [2], as well as asthmatic attacks and eye irritations. The concentrations needed to cause serious health effects, however, are rarely achieved though.

The formation of acid rain is a source of major interest and concern these days. Acid rain is caused by nitric and sulfuric acids

which are formed by the oxidation of nitrogen oxides ( $\text{NO}_x$ ) and sulfur dioxide. The increased acidity of the precipitation (down to pH about 3 in parts of New England and Europe from the "normal" pH of about 5.6) has had many deleterious effects. Many lakes have become too acidic to sustain aquatic life, most fish not being able to live with a pH below 4.5 [3]. The acidity also affects the plant life, both by attacking the leaves and branches of the vegetation and by leaching many of the nutrients in the soil into the runoff. It also has its effects on buildings and statues. Many older structures, especially those constructed of sandstone or marble, are literally dissolving.

Knowledge of a problem's existence is not always the same as understanding its cause or how to prevent it. Simplistically, sulfuric acid is formed by the oxidation and dissolution of  $\text{SO}_2$ ,



But the concentration of sulfate present in the atmosphere is much greater than that which can be accounted for by the preceding reaction [1]. Clearly, additional mechanisms for the oxidation of  $\text{SO}_2$  must play an important role in the atmosphere.

### C. $\text{SO}_2$ Oxidation Mechanisms

The proposed mechanisms for the oxidation of  $\text{SO}_2$  in the atmosphere can be divided into two general categories; gas phase reactions and heterogeneous aqueous mechanisms. The aqueous mechanisms have traditionally been divided into catalyzed and uncatalyzed

reactions. The uncatalyzed reactions can be the reaction of aquated  $\text{SO}_2$  and dissolved  $\text{O}_2$  in either the presence or absence of ammonia [4-8]. The catalyzed reactions have usually been regarded as those involving the ionic species of transition metals, in particular  $\text{Fe}^{3+}$  and  $\text{Mn}^{2+}$  [5-13]. Aqueous ozone can also oxidize the  $\text{SO}_2$  [14]. Some of the rate laws of these mechanisms are summarized in Table I-1. The rates of most of these reactions are enhanced by the presence of ammonia, which helps to keep the pH alkaline.

The gas phase reactions can be divided into homogeneous reactions, photochemical reactions (including free radical mechanisms) and gas-surface reactions. Many reactions are known in these categories [15], but many of the rate constants are still under question. None of these reaction mechanisms (or combinations thereof) can account for the amounts of sulfate observed on many occasions. It is clear that some other mechanism (or mechanisms) is occurring.

#### D. Carbonaceous Particles as a Pollutant

Carbonaceous particles are a major contribution to the total atmospheric particulate burden. Carbon can account for 30 to 50 percent of the total suspended particulate mass. The major source of these particles is from the burning of fossil fuels, whether in stationary sources such as power plants and factories, or automobiles. It had been thought that most of these particles were formed by the secondary reactions of gaseous hydrocarbons, mainly by photochemical pathways. This arose from the heavy dependence on early air pollution research on the Los Angeles type smog.

Table I-1  
SO<sub>2</sub> Oxidation Rate Laws of Various Mechanisms

Mechanism	Reaction Rate Law	Reference
O <sub>2</sub>	Rate = $\frac{H_S \{k_2 + k_1 K_W / [H^+]\} K_2 k_3}{k_{-2} [H^+]^2 + k_{-1} [H^+] + K_2 k_3} P_{SO_2}$	[8]
O <sub>3</sub>	Rate = $\{k_4 [HSO_3^-] + k_5 [SO_3^{2-}]\} [O_3 \cdot H_2O]$	[14]
Fe <sup>3+</sup>	Rate = $\frac{k_6 k_7^2 H_S^2 P_{SO_2}^2 [Fe^{3+}]}{[H^+]^3}$	[11]
Mn <sup>2+</sup>	Rate = $3.67 \times 10^{-3} \Gamma - 1.17 \{ [HSO_4^-] + [SO_4^{2-}] \}^2 \{ [Mn^{2+}] - \Gamma \} / W^2$	
	where $\Gamma = \frac{k_8 H_S P_{SO_2} [Mn^{2+}]}{k_8 \{ H_S P_{SO_2} + W [Mn^{2+}] \} + 0.17}$	[10]

$$H_S = 1.24 \text{ mole/l} \cdot \text{atm}$$

$$K_2 = 6.24 \times 10^{-8} \text{ mole/l}$$

$$k_1 = 2.9 \times 10^5 \text{ l/mole} \cdot \text{sec}$$

$$k_2 = 3.4 \times 10^6 \text{ sec}^{-1}$$

$$k_3 = 1.7 \times 10^{-3} \text{ sec}^{-1}$$

$$k_5 = 7.4 \times 10^8 \text{ l/mole} \cdot \text{sec}$$

$$k_7 = 1.84 \times 10^{-2} \text{ mole/l}$$

$$W = [H_2O(l)] \text{ in cc/m}^3$$

$$K_W = 1.00 \times 10^{-14}$$

pressure in atm, conc in mole/l

$$k_{-1} = 2.3 \times 10^{-7} \text{ sec}^{-1}$$

$$k_{-2} = 2.0 \times 10^8 \text{ l/mole} \cdot \text{sec}$$

$$k_4 = 1.1 \times 10^5 \text{ l/mole} \cdot \text{sec}$$

$$k_6 = 1.52 \times 10^2 \text{ l/mole} \cdot \text{sec}$$

$$k_8 = 8.12 \times 10^4 \text{ l/mole} \cdot \text{sec}$$

It has become evident in recent years that primary carbonaceous particle emissions are an important contribution to the total [16]. This was shown by the development of a technique to measure the light absorbing properties of the aerosol. The absorbing portions of the aerosol are the black, graphite-like soot particles, which can be formed only by the incomplete combustion of fuels. This "graphitic" component of the aerosols was found to occur with approximately the same relative concentration in many urban sites in the United States, under conditions of both low and high photochemical activity.

The structure of the graphitic particles has been studied. The diameter of these particles varies from 50 Å or even smaller to several thousand Å. The results of X-ray diffraction [17] have shown that each particle is made up of a large number of crystallites 20 to 30 Å in diameter. Each crystallite consists of several carbon layers with a graphitic structure, having defects, dislocations and discontinuities in the layer planes, thus containing high concentrations of unpaired electrons which constitute active sites. The carbon atoms located at these sites show strong tendencies to react with other molecules because of residual valencies. During particle formation, interactions of air, water, flue gas, etc., with the carbon particles can occur, resulting in the incorporation of oxygen, hydrogen and nitrogen into the structure. Nearly every type of organic functional group known has been suggested as existing at the surface of these particles. This structure is very similar to that of activated amorphous carbon.

### E. Activated Carbon

The structures of these carbons make them extremely porous; this allows large areas of the surface to be activated. It is these activated surface sites which are capable of either phys- or chem-adsorbing certain species from either gases or liquids. Because of these adsorbing properties, activated carbon has been used as a scrubber for gases and organic molecules in many processes. It is also used as a catalyst in industry for the control of gaseous emissions from smoke stacks.

An important use of activated carbon scrubbers is for the removal of sulfur dioxide from flue gas. Many industrial-style studies of the scrubber system have been performed and optimal parameters for efficiency of operation deduced [18]. It was known that these scrubbers oxidize the  $\text{SO}_2$  to sulfates, but reaction mechanisms and kinetics were never fully studied.

### F. Soot as an $\text{SO}_2$ Oxidation Catalyst

With the similarities of carbonaceous soot particles and activated carbon, it would seem reasonable that the soot could be a catalyst for the oxidation of sulfur dioxide. The possible importance of this reaction is evident in much of the collected ambient data.

During the ACHEX (California Aerosol Characterization Experiment) studies, excellent correlations between the particulate concentrations of sulfate and carbon were seen [19]. These studies were done on diurnal samples, that is, the samples were time resolved during the day to either one or two hours. Similar correlations are seen in daily sample data, collected in many urban sites in the United States,

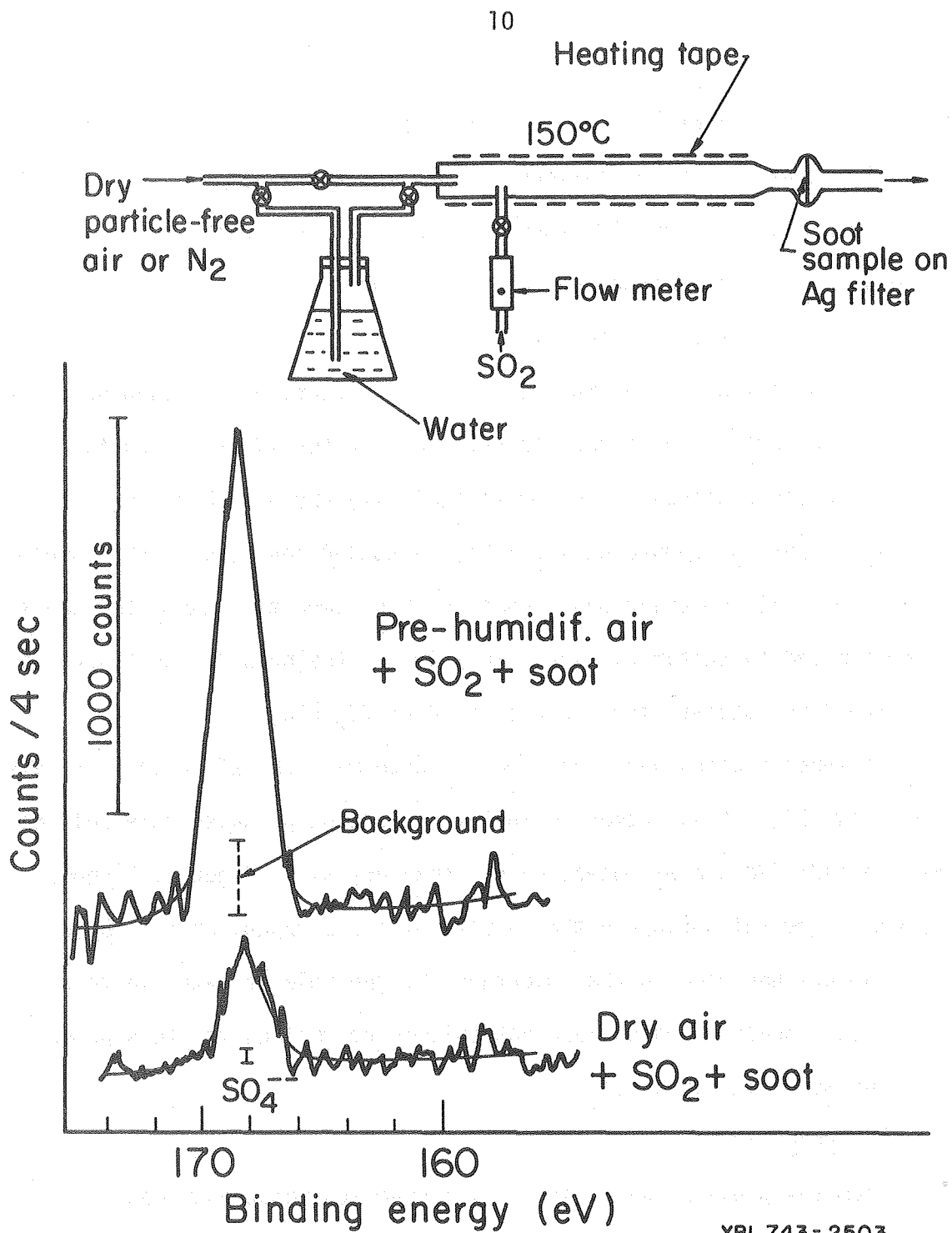
though the agreements are not as strong [20]. While it is certainly possible that these correlations are due to concurrent fluctuations of all the pollutants, greater emphasis can be placed on this correlation because the gaseous concentrations of  $\text{SO}_2$  do not correlate as well with the carbon and sulfate data.

An indication of the importance of this reaction was found quite by accident [21]. An attempt to produce a sulfur(IV) standard for ESCA (Electron Spectroscopy for Chemical Analysis), by adsorbing  $\text{SO}_2$  onto activated carbon, showed only a S(VI) photoelectron peak in the sample spectrum. This behavior was also seen when combustion generated soots were exposed to sulfur dioxide. This led to the proposal that soot was an effective catalyst for the oxidation of  $\text{SO}_2$  [22].

In studies which were performed to determine the efficiency of this reaction [23], it was observed that the reaction produced more sulfate when humidified air was used, rather than dry air. Figure 1.1 shows the experimental setup and the results of those experiments. These experiments underscored the importance of the role of water in this reaction. Reaction rates were not able to be derived for this process, nor any mechanism proposed.

#### G. Objective

From the previous work, it is clear that carbonaceous-soot particles, as well as activated carbons, are catalysts for the oxidation of sulfur dioxide. The importance of this reaction atmospherically depends on the rate of reaction and the role which liquid water plays. In the atmosphere, liquid water is important because it may condense on soot particles in stack plumes or in fog and clouds.



XBL 743-2503

Figure 1.1 Apparatus and results of experiments to study the interaction of  $\text{SO}_2$  with soot particles collected on filters.  $[\text{SO}_2] \sim 300$  ppm. Reprinted by permission of T. Novakov and S. G. Chang.

Estimated values for the concentration of carbon particles in atmospheric droplets range from 10 mg/l in a fog or cloud to as much as 10 g/l as the liquid evaporates [24].

It is the objective of this research to characterize the kinetics of the catalytic oxidation of sulfur dioxide on activated carbons in aqueous suspension. A kinetic rate law is derived for the reaction and a possible mechanism is proposed. The results indicate that this reaction could be of major importance in the formation of atmospheric sulfate.

#### H. Note on Nomenclature

Hydrated sulfur dioxide ( $\text{SO}_2 \cdot \text{H}_2\text{O}$ ) is also known as "sulfurous acid" ( $\text{H}_2\text{SO}_3$ ), but this molecule has never been observed. Within this work, the term "sulfurous acid" will be used to signify all of the sulfur(IV) containing species in solution ( $\text{SO}_2 \cdot \text{H}_2\text{O}$ ,  $\text{HSO}_3^-$  and  $\text{SO}_3^{2-}$ ). Meta-bisulfite,  $\text{S}_2\text{O}_5^{2-}$ , which is in equilibrium with bisulfite, is treated as the latter because of the concentration range used in these studies;  $\text{S}_2\text{O}_5^{2-}$  concentration does not become important until  $[\text{HSO}_3^-] > 10^{-2}$  M. The symbol S(IV) and the formula  $\text{H}_2\text{SO}_3$  are used in a similar fashion. The symbol  $\text{C}_x$  is used to signify the carbonaceous particle surface, while the term "carbon" refers to the particles of activated carbon or soot, and not the element C. The "concentration" of a carbon-particle suspension is defined as the mass of particles placed into a given volume of solution.

## II. EXPERIMENTAL

### A. Basic Setup

The kinetics of the oxidation reaction was studied with systems containing various concentrations of S(IV) and suspended carbonaceous particles. The basic reaction system consisted of an Erlenmeyer flask, in which carbonaceous particles were suspended in deionized water, to which was added a known amount of S(IV), usually as bisulfite. The mixture was stirred constantly with a Teflon coated magnetic stirring bar at approximately 300 rpm. Aliquots of the reaction mixture were removed, filtered and analyzed for sulfurous acid and sulfate during the course of the reaction.

The carbonaceous particle concentrations used in the suspensions ranged from 20 mg/l to 5.0 g/l, and the sulfurous acid concentration ranged from  $7.0 \times 10^{-8}$  to  $1.0 \times 10^{-2}$  M. Ion chromatography was used to monitor sulfurous acid and sulfate concentrations of less than  $10^{-4}$  M. For concentrations greater than  $10^{-4}$  M, the concentration of sulfurous acid was monitored by iodometric titrations while the sulfate concentration was followed by the barium sulfate turbidimetric method.

### B. Preparation of Carbon Suspensions

Combustion produced soots were collected by impinging the exhaust effluent of a flame into water, using the apparatus shown in Fig. 2.1. Soots from the combustion of acetylene, propane, natural gas, diesel fuel and coal were collected.

Flame conditions for the acetylene, propane and natural gas were controlled only to the point of creating a fuel-rich flame. This type

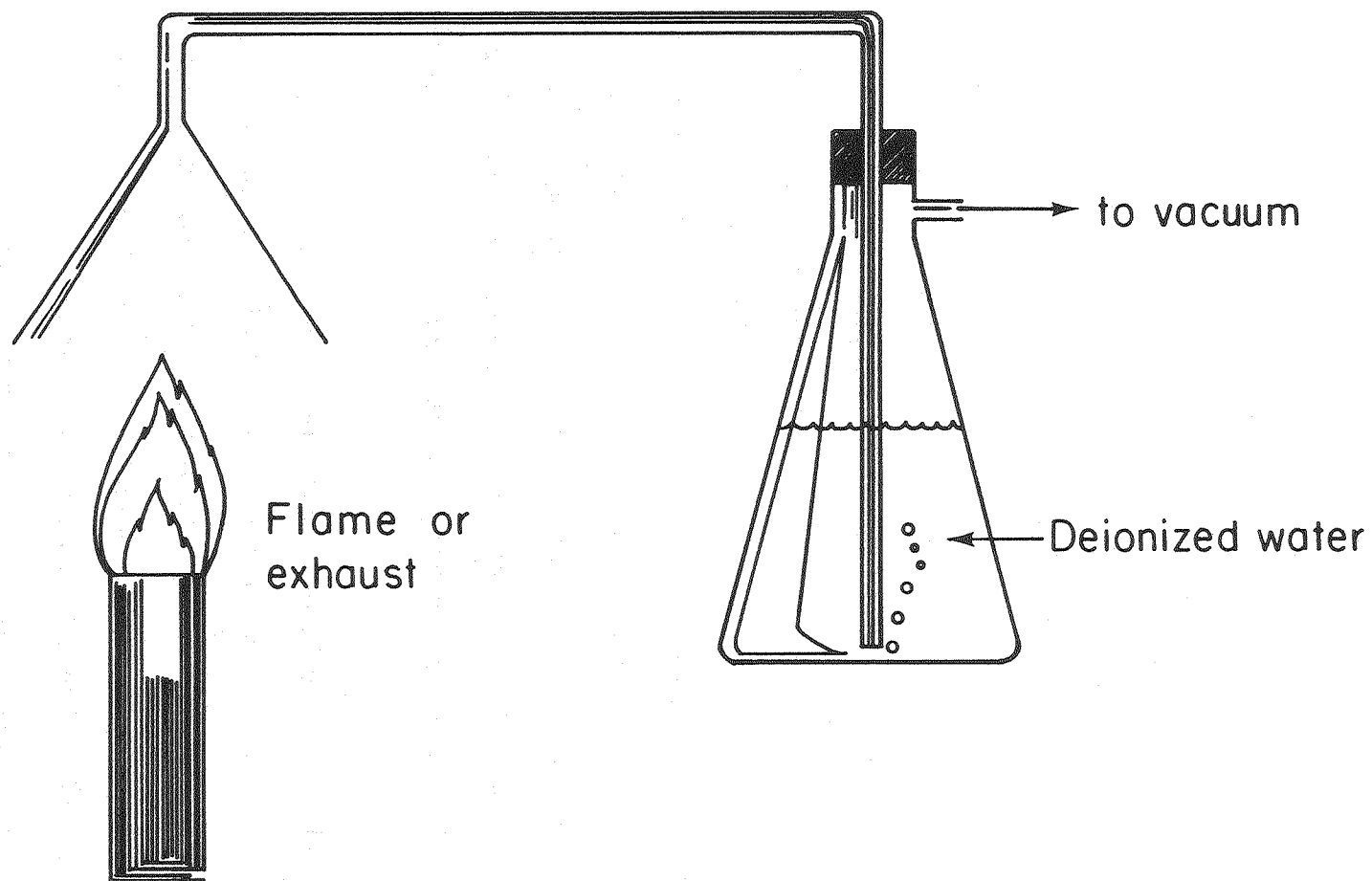


Figure 2.1 Schematic of impinger apparatus used to collect combustion-generated soots.

of flame produces more soot, because of the incomplete combustion of the fuel. The diesel soot was collected from the exhaust of a large diesel generator (a Consolidated Electric Diesel Co. Model 4260). This particular generator is rarely used and is not well tuned. While running it spews black smoke. The coal soot was collected from a coal burner using finely pulverized bituminous coal. A mechanical vibrator feeds the coal dust into a natural gas flame, and the effluent is passed through a Plexiglass chimney prior to collection [25].

The collection of combustion soots by impingement is extremely difficult. Flame and exhaust conditions constantly change and only small quantities may be collected at any given time. This irreproducibility precludes a study of the kinetic reaction using a combustion produced soot. Three different commercially available activated carbons were therefore used as model systems. These carbons were Nuchar C-190 and Nuchar S-N, manufactured by the West Virginia Pulp and Paper Co. (Wesvaco), and EM Reagents, Aktivkohle, manufactured by E. Merck [26].

The Aktivkohle is a 30-50 mesh activated carbon for use in gas chromatography. It was ground in an agate ball mill for 15 hours to produce a powder with a particle size of ~200 mesh. The two Nuchars are decolorizing carbons of 200-400 mesh. The manufacture of C-190 was discontinued in 1978. The activated carbons were washed with boiling water 3 times, to remove water soluble sulfates and nitrates that were adsorbed on the surface, and dried. This washing procedure removed the sulfate and nitrate peaks in an ion-chromatogram of the filtrate of a suspension of each carbon. Elemental analysis and physical properties of the activated carbons are shown in Table II-1.

Table II-1  
Elemental Analysis of Carbons  
weight %

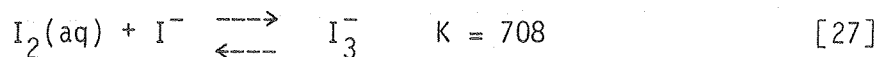
Element	C-190	SN	Aktivkohle	Tunnel	Method	
C	74.7	77.7	88.1	14.2	combustion	
H	0.9	1.56	1.60	1.75		
N	0.1	0.23	1.17	0.30		
Ca	0.221	*	0.025	1.98	XRF	
S	0.116	0.07	0.39	1.15		
Si	>0.111	*	*	>10.1		
Fe	0.117	0.011	0.018	2.83		
K	0.091	*	*	*		
Al	>0.055	*	*	>4.05		
Ti	0.016	0.0017	*	0.122		
Mn	0.013	0.0012	*	0.022		
Cr	0.002	0.0011	*	0.014		
Cu	0.002	0.0007	*	0.018		
Zn	0.002	0.0006	0.117	0.122		
Sr	0.002	*	*	0.086		
Ni	0.001	*	0.002	0.108		
Cl	0.001	*	0.001	0.101		
As	0.0004	*	*	*		
Br	0.0004	*	0.001	0.007		
Rb	0.0004	*	*	*		
Zr	0.0004	*	*	*		
Pb	0.0004	*	0.007	5.06		
Ga	0.0001	*	*	*		
Ba	*	*	*	0.158		
O	23.6	20.4	8.57	<57.8		(difference)
* below detection limits						
surface area						
[m <sup>2</sup> /g]	550	1150	1130	6		
activation						
temp °C	650	650	300			
pH (at 1g/ℓ)	5.4	7.2	6.2	5.0		
made from	coal	coal	peat	(vehicular soot)		

Automotive soot was collected in the ventilation duct above a highway tunnel. The Caldecott Tunnel is a 1.5 mile freeway tunnel on California Rt. 24, between Oakland and Orinda, running beneath the Berkeley hills. A ventilation tunnel, which runs above the roadway tunnel, has its walls coated with automotive soot. This soot was scraped from the walls using a plastic scraper into a large plastic bucket. Care was taken not to scrape concrete off the wall. The soot was then washed with boiling water 3 times and dried. The water wash removed the water-soluble organics, as well as the inorganics, which had adsorbed onto the soot surface. The composition and physical properties of the tunnel soot are shown in Table II-1.

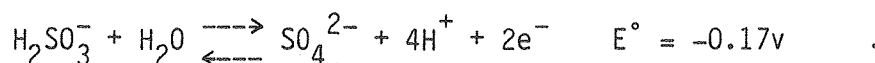
#### C. Iodometric Determination of S(IV)

The determination of the S(IV) concentrations greater than  $10^{-4}$  M was done using iodometric titrations [27]. A known amount of the reaction mixture was removed from the reaction flask and filtered using a sintered-glass filter. A known excess of standardized triiodide ( $I_3^-$ ) was added to the filtrate, along with a starch indicator. The excess triiodide was back-titrated with a standardized thiosulfate solution. Appendix A-1 shows data from a typical reaction experiment taken with this method.

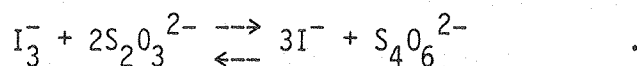
Triiodide ion is a mild oxidant and reacts quantitatively with easily oxidizable substances, such as  $H_2SO_3$ . Triiodide is formed by the reaction of molecular iodine and iodide ions,



The oxidation-reduction reactions for the determination of S(IV) with triiodide are:



The determination of S(IV) could be done by directly titrating with the triiodide; the appearance of the blue starch-triiodide complex would be the endpoint. It was found that greater precision in endpoint detection was gained, however, by observing the disappearance of the blue colored complex. Therefore, excess triiodide was added to the solution and a back-titration with standard thiosulfate was performed. The reaction of triiodide with thiosulfate is:



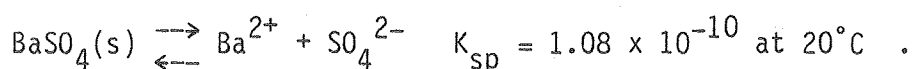
The triiodide solution was prepared by saturating deionized water over solid iodine, the solution was decanted and potassium iodide crystals were added (~1.5 g/100 ml). Typical triiodide solution concentrations were on the order of  $10^{-3}$  M.

Standard thiosulfate was prepared using sodium thiosulfate. A 0.10 N stock solution was prepared with boiled and cooled deionized water and stabilized by the addition of 1 g/l NaOH. The starch indicator was prepared by adding 5 g/l of starch (and 1.3 g/l of

salicylic acid as a preservative) to boiling deionized water. The solution is then cooled and filtered.

#### D. Turbidimetric Determination of Sulfate

The determination of sulfate concentrations greater than  $10^{-4}$  M was done by measuring the turbidity caused by the formation of barium sulfate [28]. Barium sulfate is very insoluble,



The addition of barium ion to a solution containing sulfate causes a white precipitate to form. This precipitate remains in a homogeneous suspension long enough to allow a spectroscopic determination of the turbidity of the solution. The attenuation of light due to this turbidity, read as an absorbance, has a linear relationship with the concentration of the precipitate formed (Beer's law). This permits the determination of the amount of sulfate originally in solution. Sulfite ion also forms a precipitate with barium, but can be eliminated as an interferent by making the solution acidic (pH~3) prior to the addition of the barium ion solution.

A saturated solution of  $\text{BaCl}_2$  was prepared as the source of barium ions. An aliquot of the reaction solution, after removal from the reaction flask, was filtered and 3.0 ml of the filtrate was placed in a 0.5 inch cuvette. 1.0 ml of 1 M HCl and 2.0 ml of the barium chloride solution was added, the solution mixed and the turbidity determined. Spectroscopic measurements were performed on a Bausch & Lomb Spectronic 20 at 500nm. Appendix A-1 shows the data taken in this method for a typical experiment.

### E. Ion Chromatography

Ion chromatography was used for the determination of sulfurous acid and sulfate concentrations of less than  $10^{-4}$  M. This is a technique where ions in solution are separated, using ion exchange columns, and are detected by changes in the conductivity of the eluent.

Ion exchange has been known for more than a hundred years, and many applications have been developed for it, such as softening or deionizing water and separation and purification of radio-nuclides and rare-earths, for example. With the more recent developments in high pressure liquid chromatography and conductivity detectors, systematic analysis of solutions containing many ionic species has become feasible.

Analysis was done on a Dionex Model 14 ion chromatography system, as diagrammed in Fig. 2.2. The system's columns are a 3 x 50mm concentrator, 3 x 150mm guard or pre-column, 3 x 500mm separator and a 6 x 250mm suppressor. The eluent was a 0.002 M NaOH-0.0035 M  $\text{Na}_2\text{CO}_3$  solution. The system was run at a flow rate of 138 ml/h and at a pressure of 600 psi.

The ion exchange resin in the first three columns is an anion exchange resin of the form  $\text{R}^+\text{HCO}_3^-$  or  $\text{R}^{2+}\text{CO}_3^{2-}$ . The concentrator column can be taken out of line of the eluent flow, by the injector valve, and a known volume of sample injected in to it. The anions of the sample replace the carbonate and bicarbonate ions on the resin. When the column is placed back into the eluent flow, the carbonate in the eluent will exchange with the sample anions and an ionic separation will occur, according to the affinity each anion has for the ion

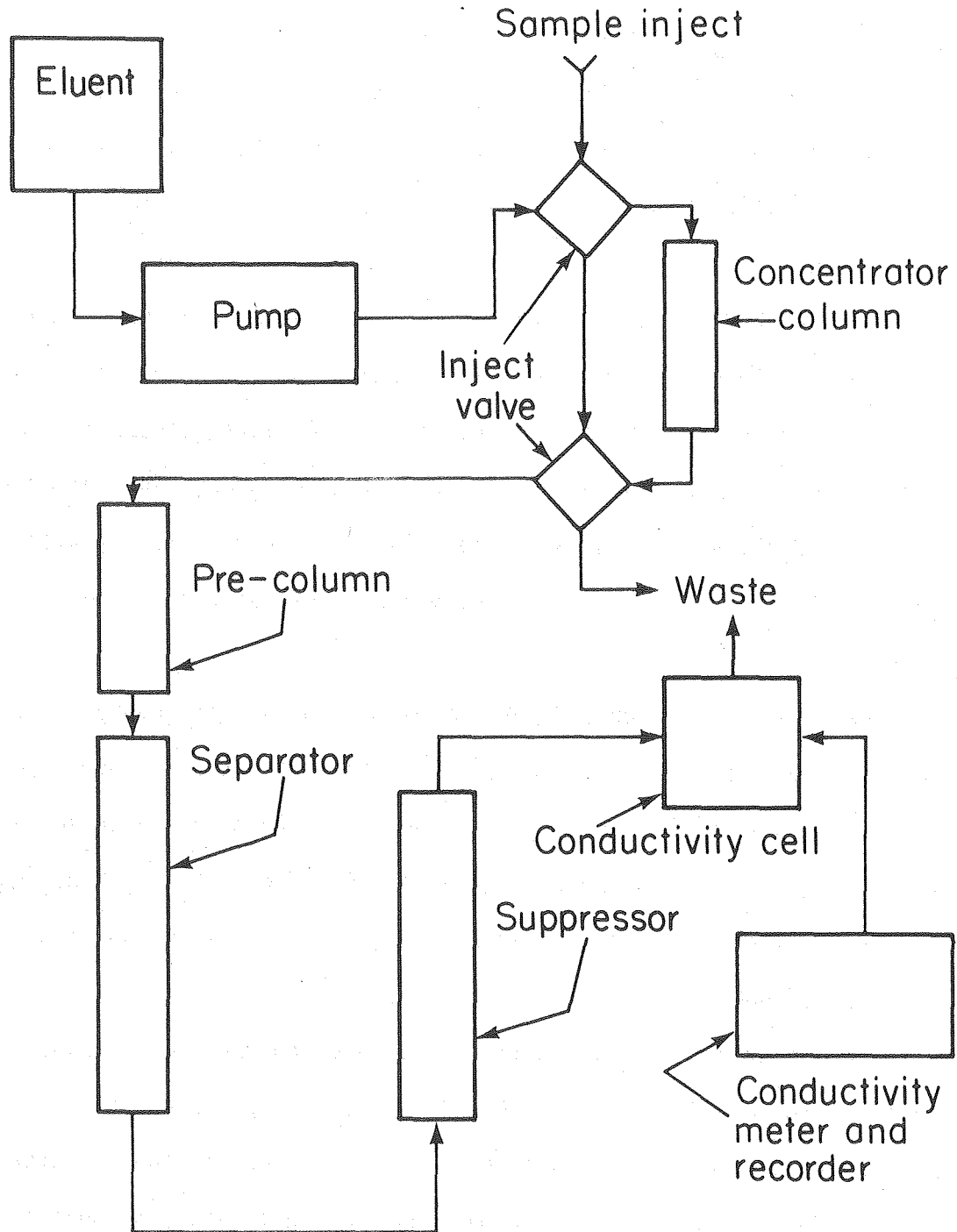


Figure 2.2 Schematic of ion chromatography system.

XBL8010-2277

exchange resin. The short precolumn is used to protect the larger separator from dirt and contamination. (The pre-column costs about \$150, the separator \$600.)

The suppressor column contains a cation exchange resin, of the form  $\text{RSO}_3^-\text{H}^+$ . As the eluent passes through the suppressor, the sodium ions in solution exchange with the hydrogen ions. The effluent of the columns is  $\text{CO}_2 \cdot \text{H}_2\text{O}$  (under pressure) and the sample ions are converted to their acid forms. The conductivity of most of the acids is greater than that of carbonic acid, which has a very low conductivity, and can therefore be detected in the conductivity cell. For the low values of specific conductance being measured ( $0.01 - 50.0 \cdot 10^{-6} \text{ ohm}^{-1} \text{ cm}^{-1}$ ), concentration of a given species is linearly proportional to its conductivity.

Reactions were followed by removing an aliquot of the reaction mixture and filtering through a washed Whatman 41 paper filter in a Buchner funnel. The filtrate was then injected onto the concentrator column through an in-line 12.5mm Millipore filter (pore size  $0.22 \mu\text{m}$ ) which had been washed and sonicated to remove any ionic contaminations. Appendix A-2 shows data from a typical experimental run taken with this method, along with a sample chromatogram and calibration data.

It has been reported [29] that sulfite oxidizes to sulfate in the chromatographic system and an oxidation inhibitor must be added if sulfite and sulfate are to be determined. These inhibitors include isopropanol, formaldehyde and thiosulfate. Use of one of these inhibitors will change the conductivity and all standards and samples would have to be done with equal inhibitor concentrations. Injection

of a standard sulfite solution into our system without an inhibitor, however, did not produce a sulfate peak. After many months of equipment use, for many different types of experiments, sulfite oxidation was seen to occur. Cleaning and reconditioning of the columns, by the methods recommended in the Dionex instrument manual, avoided the oxidation.

It appears that contamination of the concentrator column and pre-column can occur when solutions containing manganese and arsenic salts are injected through the anion system. These trace contaminants are enough to oxidize the injected sulfite, but are removed by completely reconditioning the columns. This behavior has now been confirmed by other users of ion chromatographs [30,31].

#### F. Miscellaneous Techniques

All reactions, except for those in which temperature or dissolved oxygen concentration were specifically controlled, were done at room temperature (20°C) and open to the air (dissolved  $O_2 = 2.64 \times 10^{-4}$  M). Oxygen-dependence studies were performed in a contained atmosphere glove box with various mixtures of  $N_2$  and  $O_2$ . The gaseous oxygen concentrations ranged from 5 to 48 percent, with the remainder of the gas being pure nitrogen. The dissolved  $O_2$  was equilibrated by vigorously shaking the water to be used and then bubbling the  $N_2-O_2$  mixture through the water. Known amounts of activated carbon and sulfurous acid were then added to form the reaction mixture.

Oxygen-dependence studies were done with the S(IV) concentrations between  $10^{-4}$  and  $10^{-3}$  M. This allowed the S(IV) concentration to be measured by the iodometric technique, which was performed in the

glove box. This eliminated any contact of the reaction mixture or filtrates with air. The dissolved oxygen concentration was measured with a Yellow Springs Instrument Model 57 dissolved oxygen meter.

Temperature-dependence (activation energy) studies were performed by immersion of the reaction flask in a controlled temperature bath. The temperatures used ranged from 5 to 50°C. A few experiments were performed using activated carbon that had been degassed. The carbon was degassed by exposure to vacuum (0.1 Torr) at 75°C for three days. One atmosphere of N<sub>2</sub> was then introduced for 24 hours.

The pH of the solution was adjusted by the addition of H<sub>2</sub>SO<sub>4</sub> to SO<sub>2</sub>·H<sub>2</sub>O for pH < 2.5, and various combinations of SO<sub>2</sub>·H<sub>2</sub>O, NaHSO<sub>3</sub>, Na<sub>2</sub>SO<sub>3</sub>, NH<sub>4</sub>OH, and NaOH were used to control the pH above 2.5. The pH was measured using a Beckman digital pH meter with combination probe. Buffer solutions of other inorganic or organic acids were not used, because of the possibility of interferences and inhibition of the reaction by the buffer species. To study the possible interferences and inhibition of the reaction by other pollutants present in atmospheric droplets, water was condensed from the Berkeley atmosphere on clear and foggy days, and then used to make the reaction mixture. Collected rain water was also used.

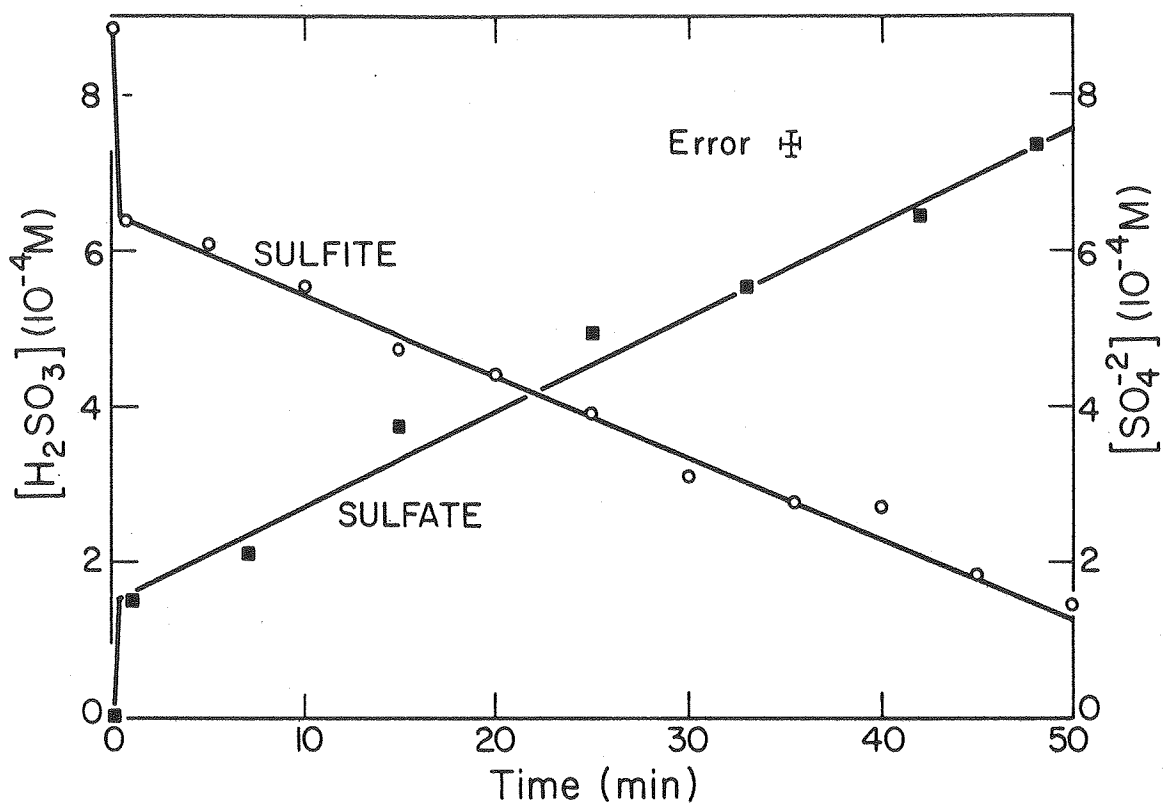
### III. RESULTS

#### A. Activated Carbons: The Reaction and S(IV) Dependence

The oxidation of S(IV) to sulfate on activated carbon is demonstrated in Fig. 3.1. This figure is a plot of the data of Appendix A-1, with Nuchar C-190 as the activated carbon used. The results shown are typical of the oxidation of sulfurous acid with all of the carbons used. For the concentration range shown ( $[S(IV)]$  between  $10^{-4}$  and  $10^{-3}$  M), the reaction appears to proceed in two distinct steps. These are an initial rapid oxidation of the sulfurous acid followed by a slower, linear oxidation. The decrease in  $H_2SO_3$  concentration is matched by a corresponding increase in sulfate concentration, which shows that oxidation of the S(IV) is indeed occurring.

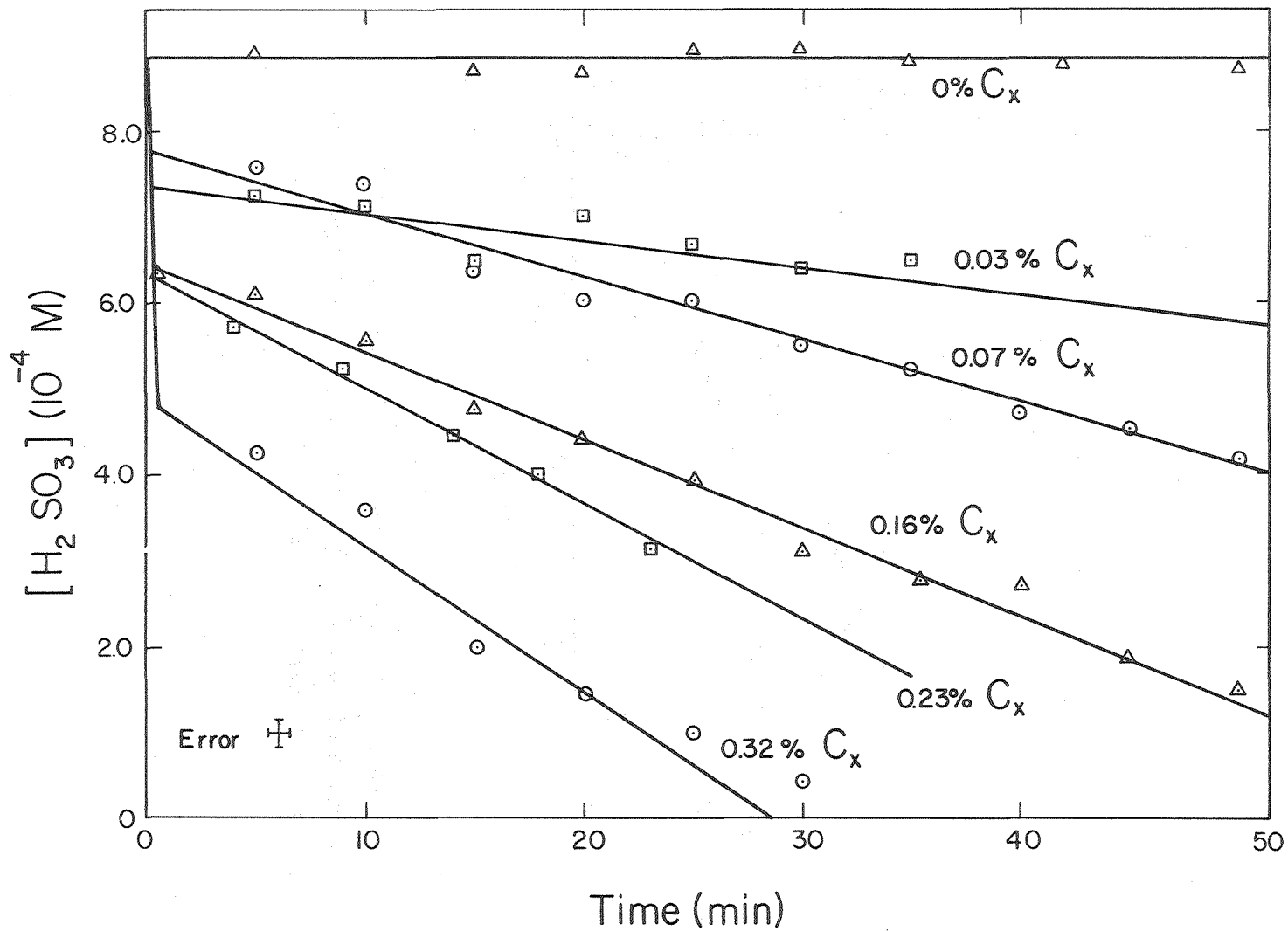
The effects of varying the "concentration" of the carbon in suspension on the reaction rate are shown in Fig. 3.2. As the "concentration" of the carbon increases, so does the rate of oxidation. Also of interest in this figure is the "blank" reaction, i.e., where no carbon catalyst was present. The curve shows that for the S(IV) concentration and periods of time involved, no significant oxidation occurs in the absence of the carbon catalyst. Also shown in this figure, though not as clearly, is that as the carbon concentration increases, so does the magnitude of the initial rapid oxidation.

The rate of the slower, linear reaction as a function of carbon concentration is shown in Fig. 3.3. Here it is seen that for carbon concentration of 0 to 4 g/l, the rate of sulfate formation is proportional to the concentration of the suspended activated carbon. This



XBL 782-219

Figure 3.1  $\text{H}_2\text{SO}_3$  and  $\text{SO}_4^{2-}$  concentrations versus time for a 1.6 g/l suspension of Nuchar C-190. Curves are least squares fit to "slower oxidation" data.



XBL7911-13278

Figure 3.2  $\text{H}_2\text{SO}_3$  concentration versus time for various concentrations of Nuchar C-190 suspensions. Carbon concentrations expressed as weight % of solution. Curves are least squares fit to "slower oxidation" data.

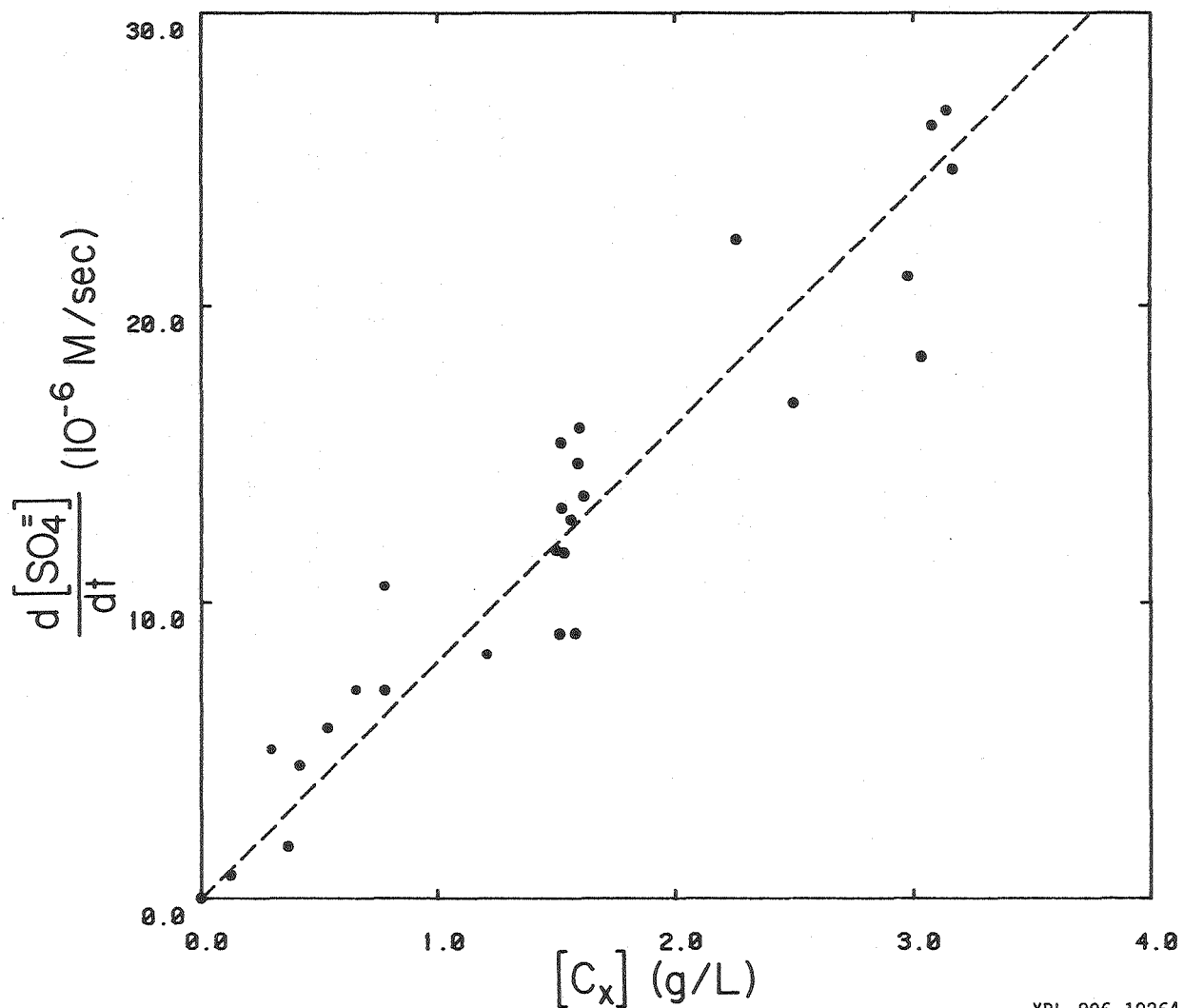


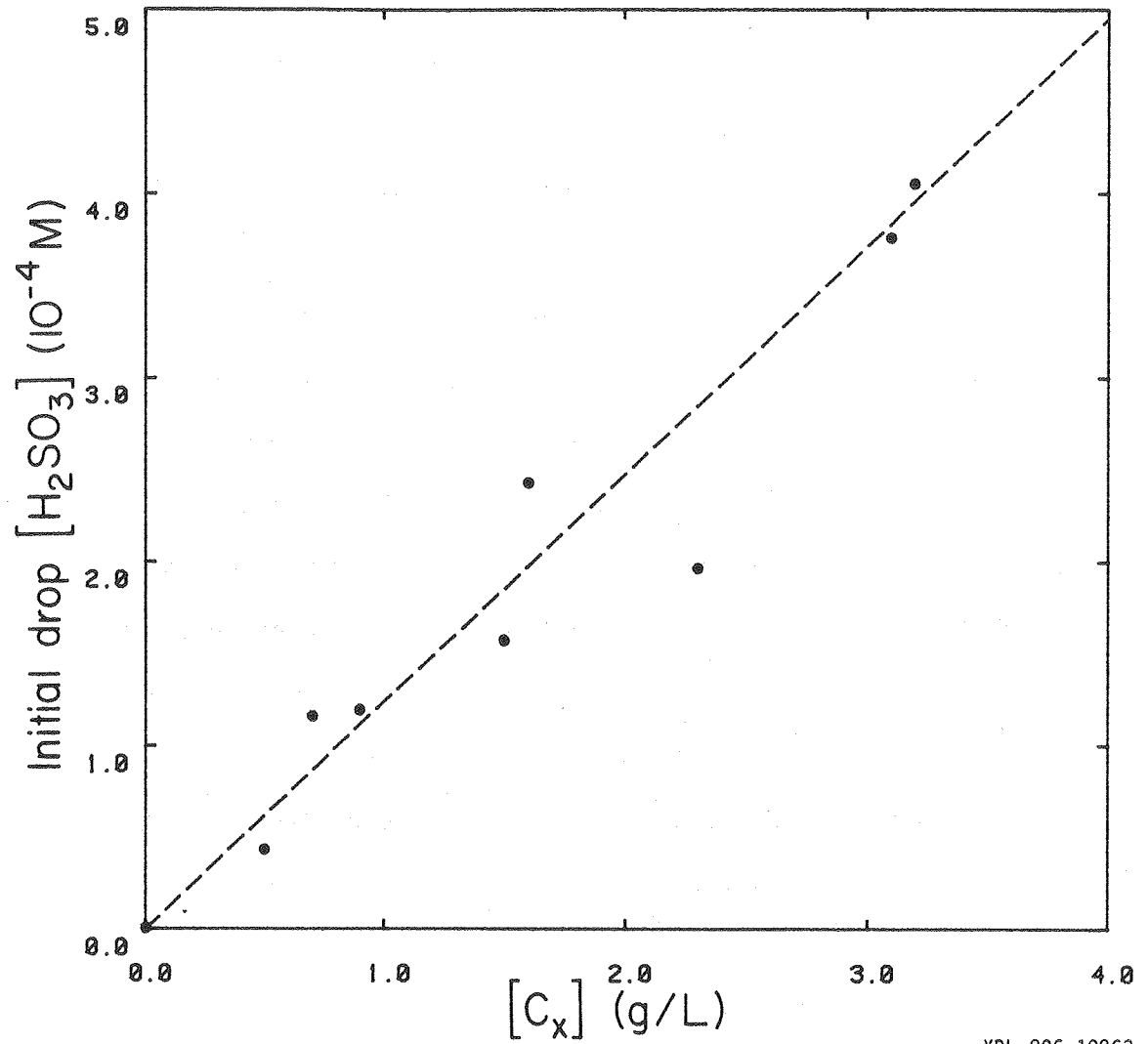
Figure 3.3 Reaction rate versus suspended Nuchar C-190 concentration. Initial  $\text{H}_2\text{SO}_3$  concentration range:  $5 \times 10^{-4}$  -  $1.2 \times 10^{-3}$  M. Curve is least-squares fit of data.

XBL 806-10264

figure shows data for Nuchar C-190 when the initial  $\text{H}_2\text{SO}_3$  concentration is between 0.5 and  $1.2 \times 10^{-3}$  M. Since the oxidation of S(IV) is a linear function of time (Figs. 3.1-2) when the S(IV) concentration is greater than  $10^{-4}$  M (i.e., zeroth order dependence of rate on S(IV)), no corrections for the S(IV) concentration on the sulfate formation rate are needed.

The magnitude of the initial rapid oxidation is plotted as a function of activated carbon concentration in Fig. 3.4. Again, a linear proportionality is seen with activated carbon concentrations. Studies of only the magnitude of this initial oxidation proved to be possible with the analytic techniques used. It was found that whenever activated carbon was added to a solution containing a known concentration of sulfurous acid, no matter how fast the analysis (<0.5 min), the initial oxidation had already occurred.

The rapid oxidation was able to be eliminated by two methods. The first was by placing the activated carbon into the water first, and after allowing the carbon and water to mix for a few minutes, then adding a known amount of sulfurous acid. The second was by degassing the carbon in vacuum and then saturating it with nitrogen. If the carbon is then quickly transferred into a solution containing S(IV) no initial rapid oxidation will occur. Conversely, if the activated carbon is allowed to equilibrate with an oxygen-nitrogen mixture where the partial pressure of oxygen is greater than that in air, the magnitude of the initial rapid oxidation increases. The behavior of the reaction rate and the initial oxidation with respect to the carbon



XBL 806-10263

Figure 3.4 Initial drop in  $H_2SO_3$  concentration versus suspended Nuchar C-190 concentration.  $[H_2SO_3]_0 = 8.85 \times 10^{-4}$  M. Curve is least-squares fit of data.

concentration was the same for all the activated carbons and soot catalysts studied.

The behavior of the reaction rate as a function of the S(IV) concentration is shown in Figs. 3.5-3.7 for the different activated carbons used. The data shown in these plots were all taken at room temperature (20°C) and in air. The rates are normalized to a 1 g/l activated carbon concentration. (The data points are the instantaneous rates based on three-point averages from the various experiments. The details of the calculations used are discussed in Appendix B.)

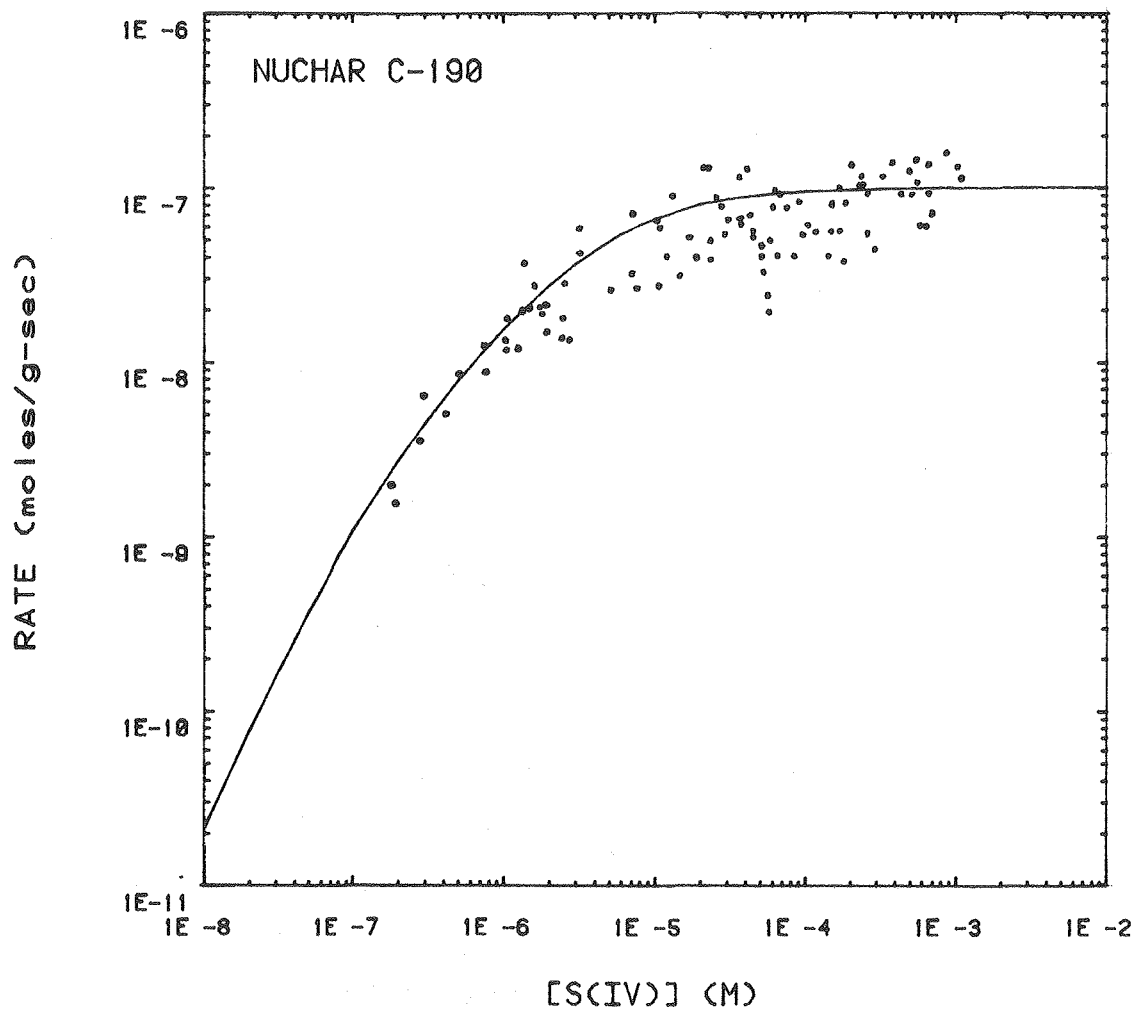
Figure 3.5 shows that, for the Nuchar C-190, the reaction rate is independent of the S(IV) concentration when that concentration is greater than  $10^{-4}$  M, and becomes increasingly dependent on the concentration as it decreases. Similar behavior is seen in Figs. 3.6 and 3.7 for the Nuchar SN and the Aktivkohle.

Though the data for each activated carbon are different, each set can be fit with the equation:

$$y = k \cdot \alpha x^2 / (1 + \beta x + \alpha x^2) \quad , \quad (\text{III.1})$$

where  $y = \text{rate} \equiv d[\text{S(IV)}]/dt \div [C_x]$  and  $x = \text{S(IV) concentration}$ .

This equation states that the rate will be second order with respect to S(IV) when  $1 \gg \beta x + \alpha x^2$ , independent of S(IV) when  $\alpha x^2 \gg \beta x + 1$  and having an order between zeroth and second when the terms of the quadratic in the denominator are of comparable magnitudes. This changing order of the dependence can also be seen as the "slope" of the curves in the log-log plots of Figs. 3.5-3.7 (i.e., if  $y = kx^n$ ,



XBL 8010-12605

Figure 3.5 Normalized rate of reaction versus total S(IV) concentration for NuCHAR C-190. Curve is polynomial least-squares fit of data.

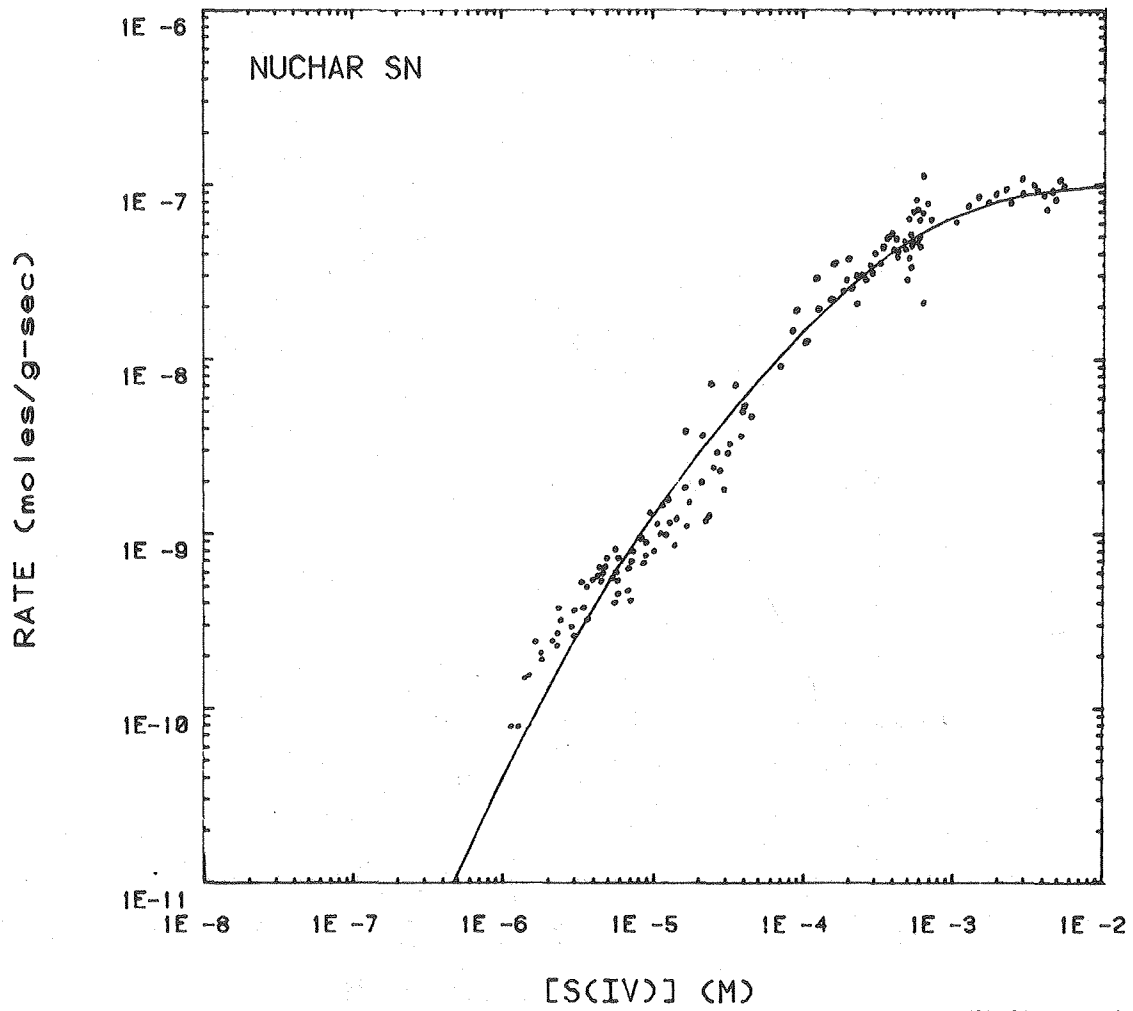
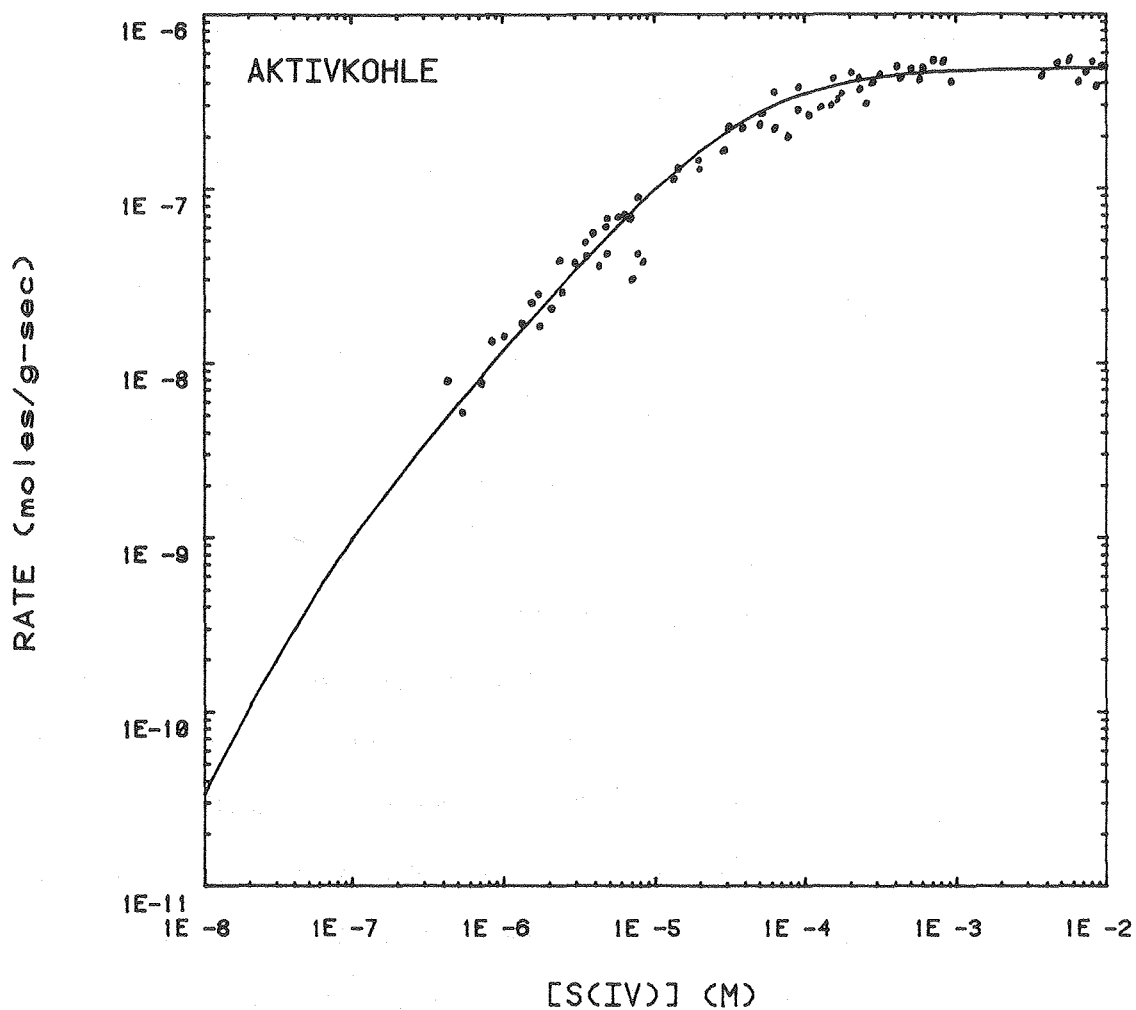


Figure 3.6 Normalized rate of reaction versus total S(IV) concentration for Nuchar SN. Curve is polynomial least-squares fit of data.



XBL 8010-12603

Figure 3.7 Normalized rate of reaction versus total S(IV) concentration for Aktivkohle. Curve is polynomial least-squares fit of data.

$\log y = n \cdot \log x + \log k$ ). For the Nuchar C-190 in Fig. 3.5, the slope of the curve shows that the rate of reaction is second order with respect to the S(IV) below  $10^{-7}$  M, moves through a first order reaction around  $5 \times 10^{-6}$  M and becomes zeroth order above  $10^{-4}$  M.

An identical type of behavior is seen in Fig. 3.8 from the reactions done with tunnel-soot scrapings as the catalyst. In this figure, the data points are normalized to the concentration of elemental carbon present as opposed to the total amount of activated carbons. This is because of the relatively small amount of carbon (14 percent) present in the soot. The values of the coefficients of equation III.1 which give the best fit curve for each set of data are shown in Table III-1.

#### B. Oxygen and Temperature Studies

The dependence of the reaction rate on dissolved oxygen concentration for the three activated carbons is shown in Fig. 3.9. As in the previous figures, the reaction rate is normalized to unit activated carbon concentration. The rates were all taken as the instantaneous rates at a sulfurous acid concentration of  $5 \times 10^{-4}$  M. This was done to eliminate the effects that the S(IV) concentration has on the rate. While the rate is not highly dependent on the S(IV) concentration in this region for the Nuchar C-190 and the Aktivkohle, Fig. 3.6 shows that for the Nuchar SN, this precaution is necessary.

The three sets of data in Fig. 3.9 can each be fit to the equation,  $y = k \cdot \gamma x / (1 + \gamma x)$ , where  $y$  = rate and  $x$  = dissolved oxygen concentration. This equation shows that the reaction rate can vary from a first order dependence with respect to oxygen when  $1 \gg \gamma x$  to zeroth order

Table III-1  
Coefficients of least-squares fit of  
rate versus S(IV) concentration data

---

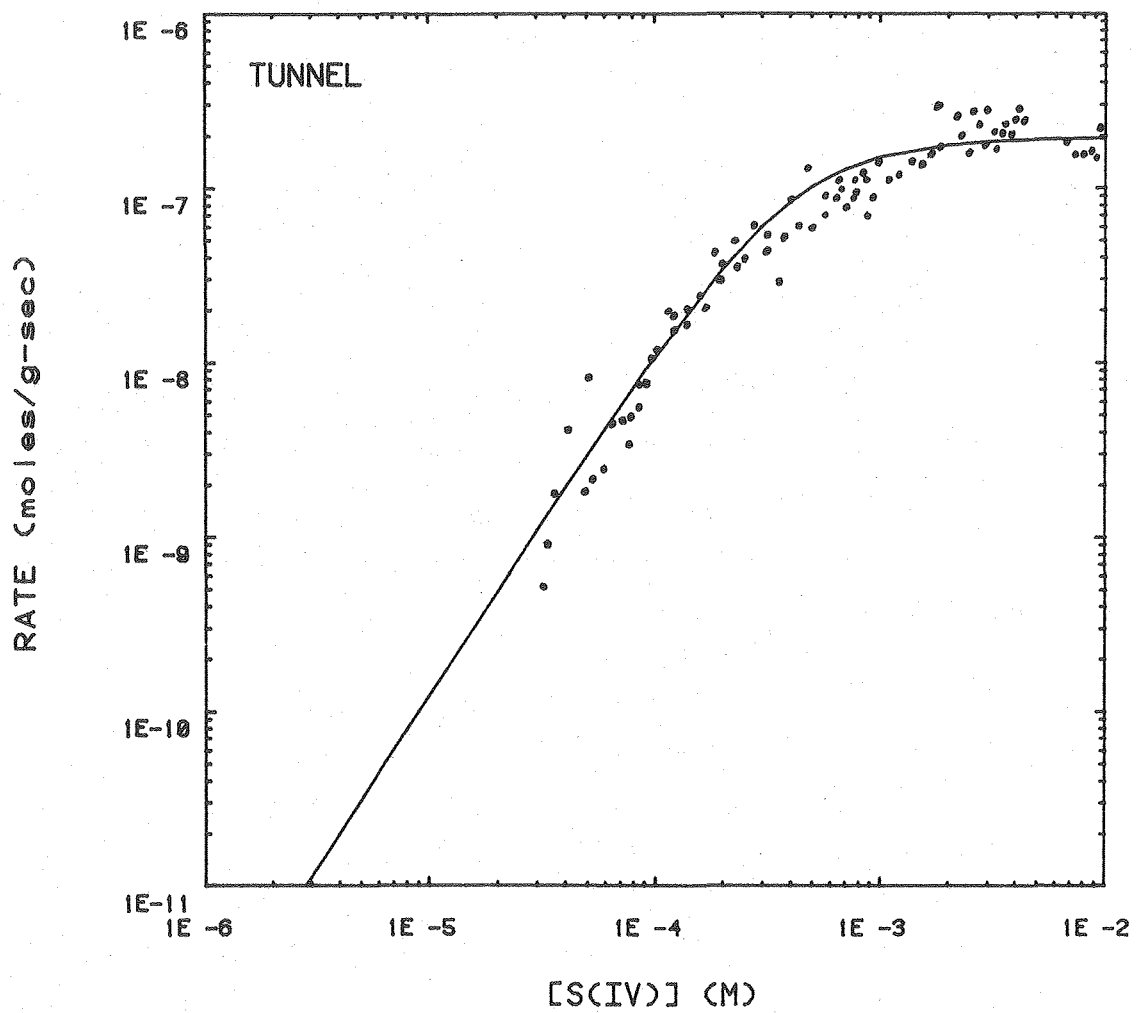

$$\text{rate} = K \frac{\alpha[S(\text{IV})]^2}{1 + \beta[S(\text{IV})] + \alpha[S(\text{IV})]^2}$$


---

	C-190	SN	Aktivkohle	Tunnel
$k(10^{-7}\text{mol/g-sec})$	1.0	1.0	4.9	2.0
$\alpha(\ell^2/\text{mol}^2)$	$2.4 \times 10^{12}$	$4.9 \times 10^8$	$9.5 \times 10^{11}$	$6.4 \times 10^6$
$\beta(\ell/\text{mol})$	$1.2 \times 10^7$	$3.0 \times 10^6$	$3.7 \times 10^7$	$9.9 \times 10^2$
$\chi^2$	59	122	33	40

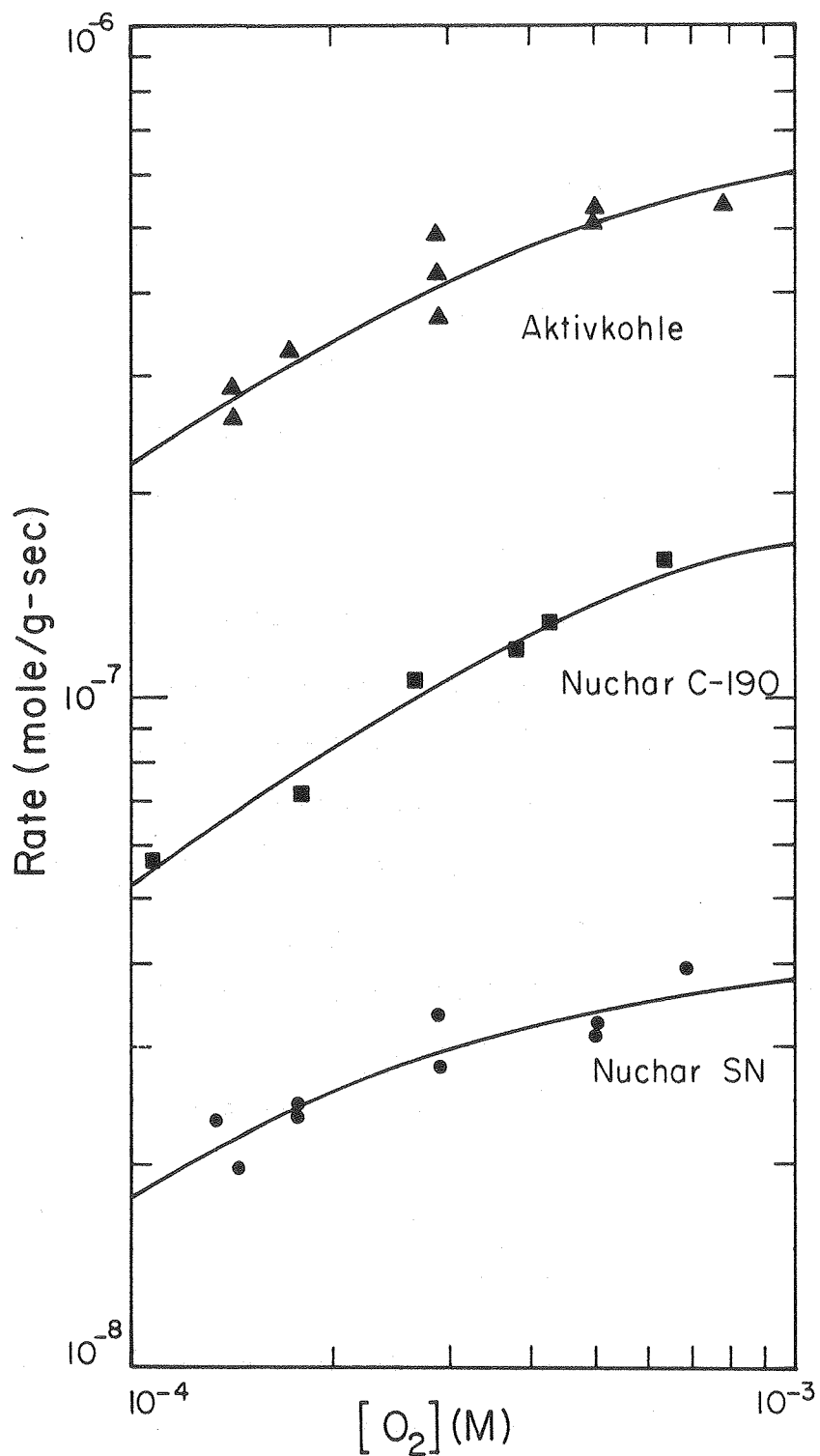
---

see Appendix B



XBL 8010-12602

Figure 3.8 Normalized rate of reaction versus total S(IV) concentration for tunnel soot scrapings. Curve is polynomial least-squares fit of data.



XBL8010-2279

Figure 3.9 Normalized rate of reaction versus dissolved oxygen concentration.  $[S(IV)] = 5 \times 10^{-4}$  M. Curves are polynomial least-squares fit of data.

when  $\gamma x \gg 1$ . The values of  $\gamma$  and the correlation coefficients for the three activated carbons are shown in Table III-2. The rate of diffusion of oxygen into solution does not affect the reaction rate, since the concentration of dissolved oxygen was determined to be constant during the course of the reaction.

The dependence of the reaction rate as a function of temperature for the three carbons is shown in Fig. 3.10. The data are being plotted to the Arrhenius equation,  $\ln k = \ln A - E/RT$ , where  $k$  is the specific rate constant at some temperature,  $T$  is the absolute temperature and  $R$  is the gas constant.  $A$  and  $E$  are empirical constants obtained from this plot, with  $E$  being the activation energy of the reaction. The reaction rates plotted have been corrected for dissolved oxygen concentration, with the data obtained in Fig. 3.9, as well as normalized for carbon and S(IV) concentrations. The oxygen correction is necessary as the solubility of oxygen is a function of temperature. The values obtained for the activation energy and the Arrhenius constant,  $A$ , are summarized in Table III.2.

For more accuracy, a corrected form of the Arrhenius equation,

$$\ln k = \ln A + (C/R)\ln T - E/RT \quad ,$$

where  $C$  has units of a molar heat capacity could be used [32]. While for many reactions in solution the factor  $C/R$  is rather large, treatment of the data obtained in these experiments in this manner shows only minor changes in the calculated activation energies and Arrhenius

Table III-2  
Summary of kinetic data for  
S(IV) oxidation on activated carbons

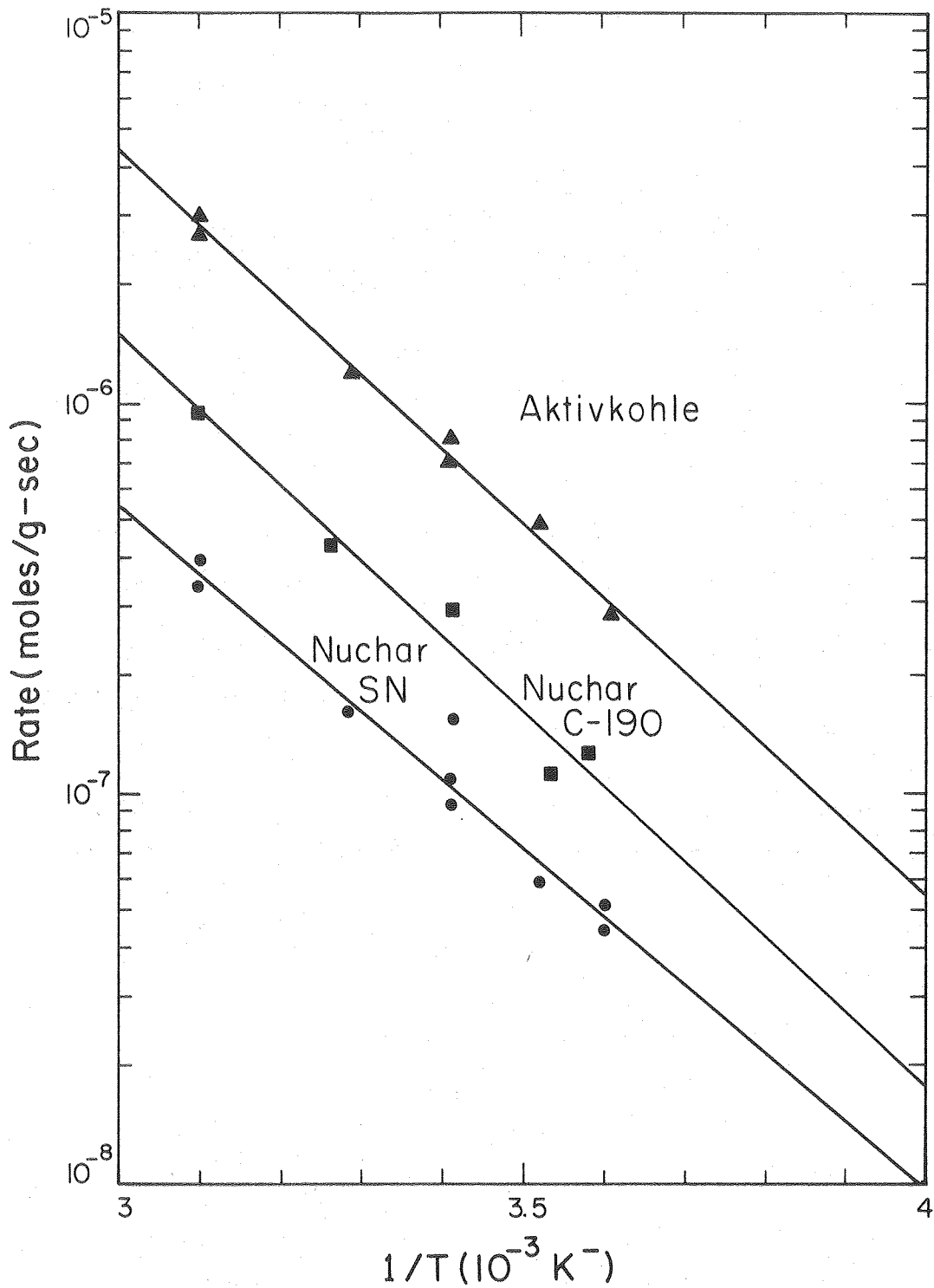
$$\frac{d[\text{SO}_4^{2-}]}{dt} = A e^{-E_a/RT} [C_x] \left\{ \frac{\gamma[\text{O}_2]}{1+\gamma[\text{O}_2]} \right\} \left\{ \frac{\alpha[\text{S(IV)}]^2}{1+\beta[\text{S(IV)}]+\alpha[\text{S(IV)}]^2} \right\}$$

	C-190	SN	Aktivkohle
A(mole/g-sec)	0.87	0.16	2.5
E <sub>a</sub> (kcal/mole)	8.8	8.1	8.8
γ(l/mole)	2.1 x 10 <sup>3</sup>	7.4 x 10 <sup>3</sup>	4.4 x 10 <sup>3</sup>
α(l <sup>2</sup> /mole <sup>2</sup> )	2.4 x 10 <sup>12</sup>	4.9 x 10 <sup>8</sup>	9.5 x 10 <sup>11</sup>
β(l/mole)	1.2 x 10 <sup>7</sup>	3.0 x 10 <sup>5</sup>	3.7 x 10 <sup>7</sup>
r <sup>2</sup> (oxygen)	0.98	0.85	0.93
r <sup>2</sup> (Arrhenius)	0.96	0.95	0.99

$$\sigma_A^2 = \pm 10 \text{ percent}$$

$$\sigma_E^2 = \pm 5.0 \text{ percent}$$

$$\sigma_\alpha^2 = \sigma_\beta^2 = \sigma_\gamma^2 = \pm 3.0 \text{ percent}$$



XBL 8010-2280

Figure 3.10 Normalized rate of reaction versus  $1/T$  (Arrhenius plot).  
Curves are least-squares fit of data.

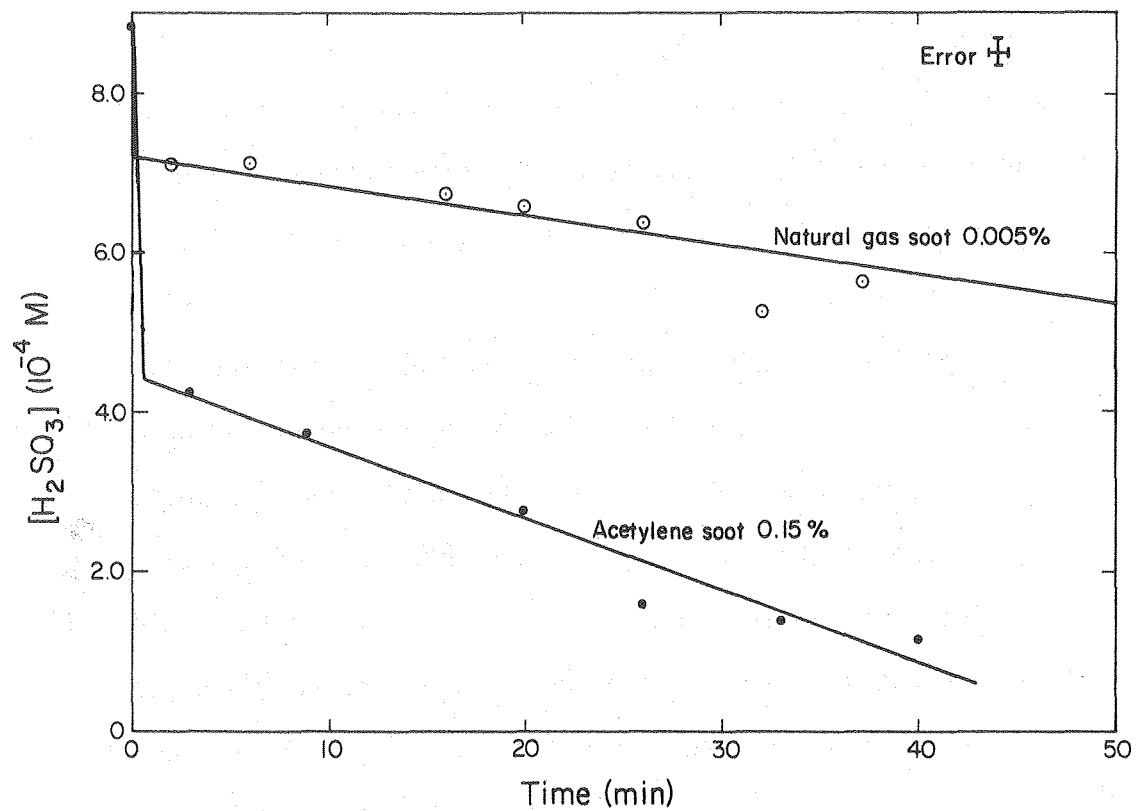
constants. Within the accuracy of these experiments (see Appendix B), the use of this correction is not warranted.

### C. Combustion-Soot Studies

Combustion produced soots show the same catalytic nature as the activated carbons. Figure 3.11 shows reaction curves for acetylene and natural gas soot suspensions. The reaction proceeds as before, with an initial rapid oxidation followed by a slower process. The concentrations of the soots are shown as weight percent of the solution of elemental carbon. Figure 3.12 shows projected reaction curves for many of the carbon catalysts studied. The initial rapid oxidation has been ignored and a catalyst suspension concentration of 0.5 g/l assumed. This figure shows the relative reactivity of the different soots and activated carbons in the region where the reaction rate is nominally independent of S(IV) concentration. Figure 3.13 shows the relative reactivity of the four carbons studied in detail over a wide range of S(IV) concentrations.

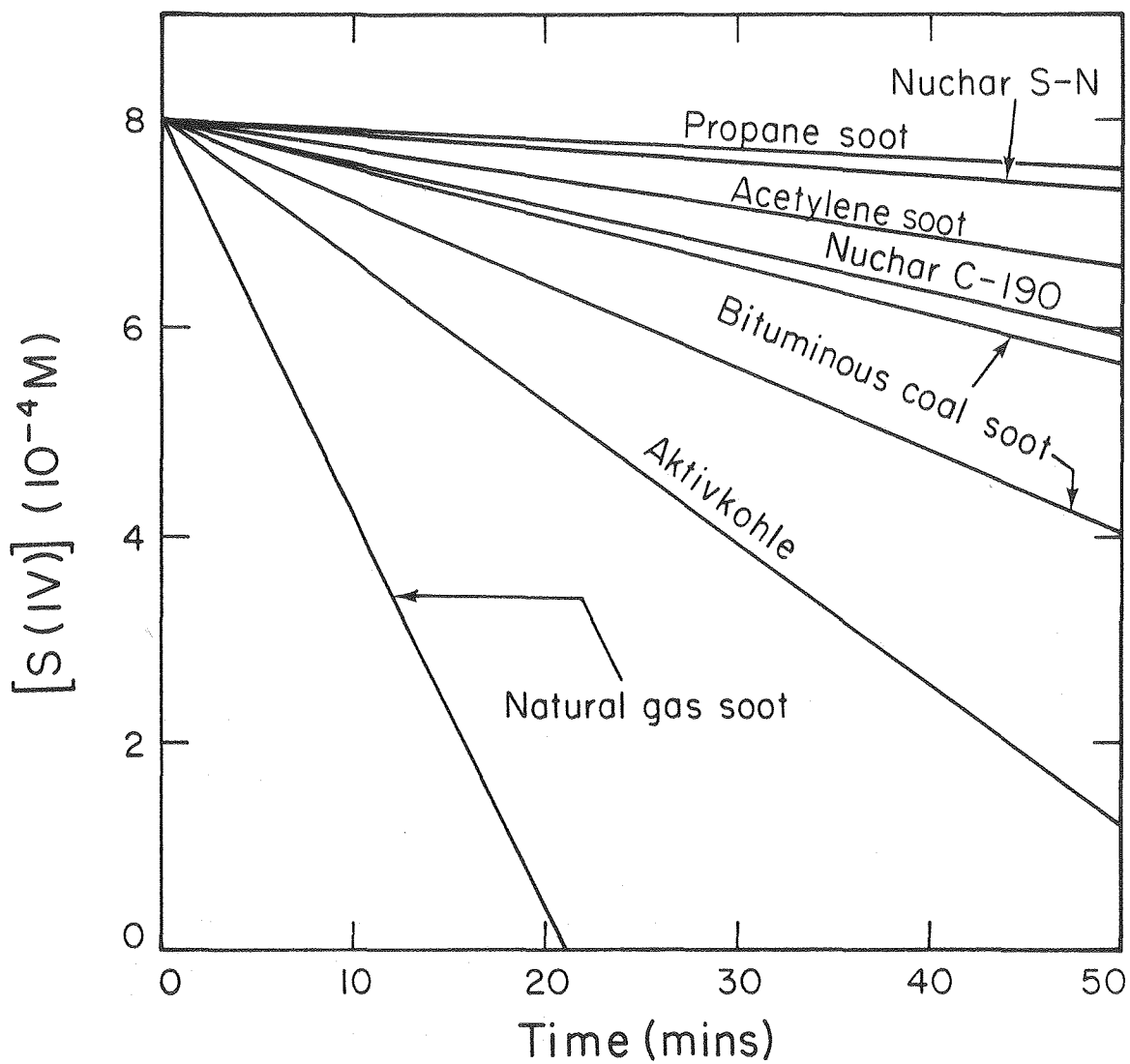
### D. pH Effects

The effects of pH on the reaction are demonstrated in Fig. 3.14. As can be seen, there is no significant difference between the reaction behavior in strong acid (pH = 1.45) to that in neutral solution (pH = 7.50). The pH values shown are the initial values of the pH. As the reaction proceeded, the solution in all cases became more acidic, with a net change normally of ~0.5 pH units. The differences between the reaction curves for the individual experiments are well within the scatter for experiments which are all done with identical



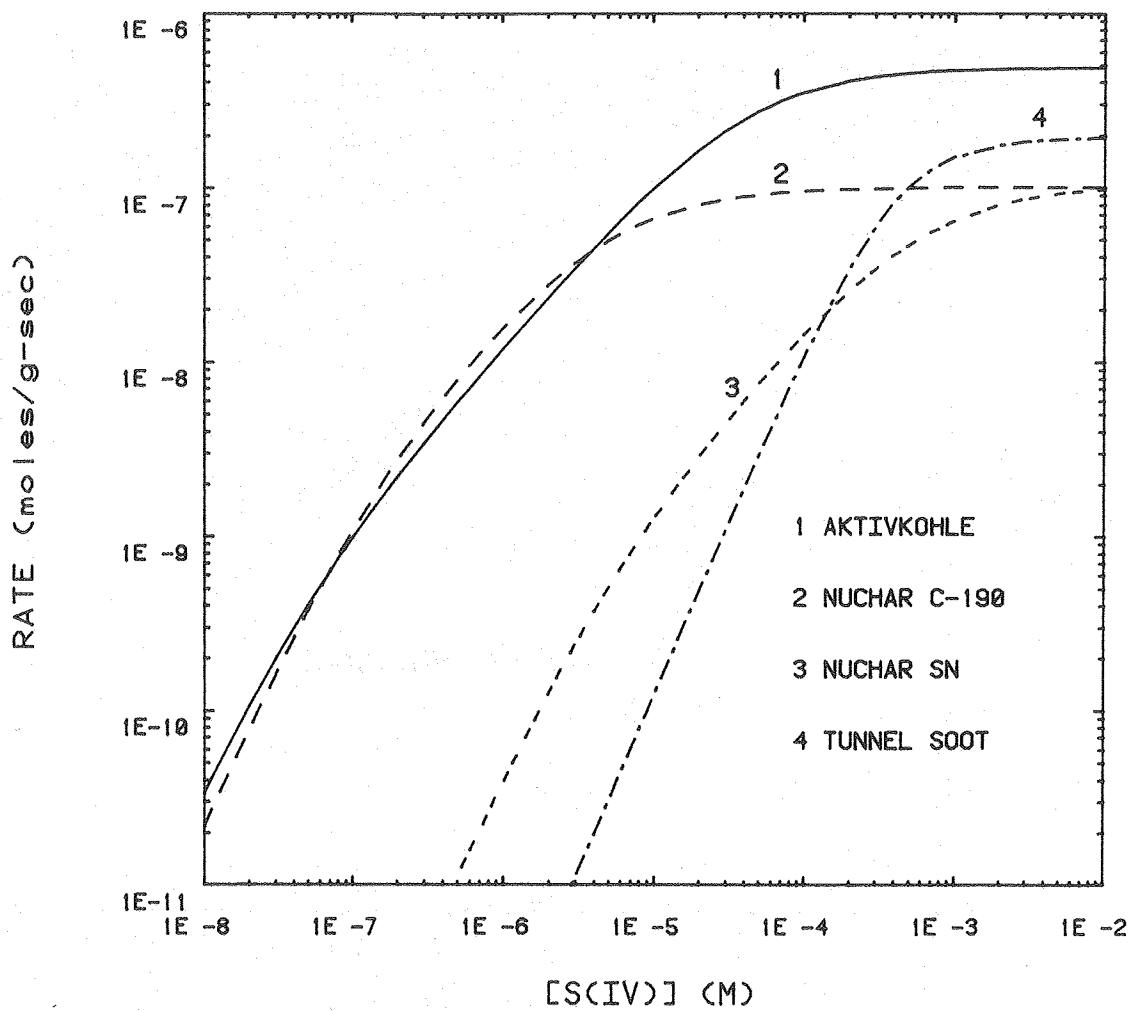
XBL7710-2065A

Figure 3.11  $\text{H}_2\text{SO}_3$  concentration versus time for acetylene and natural gas soot suspensions. Curves are least-squares fit to "slower oxidation" data.



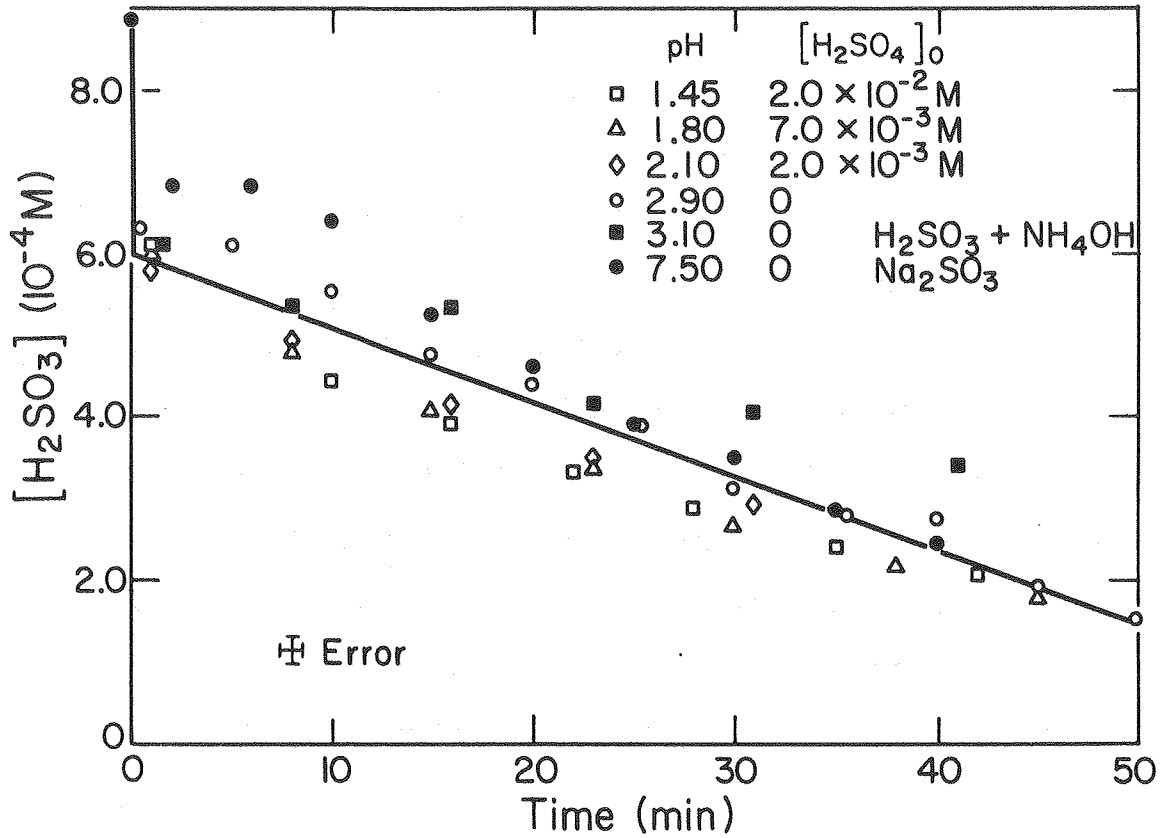
XBL8010-2278

Figure 3.12 S(IV) concentration versus time for various types of carbons and soots.  $[C_x] = 0.5 \text{ g/l}$ .



XBL 8010-12601

Figure 3.13 Normalized rate of reaction versus total S(IV) concentration for various catalysts.



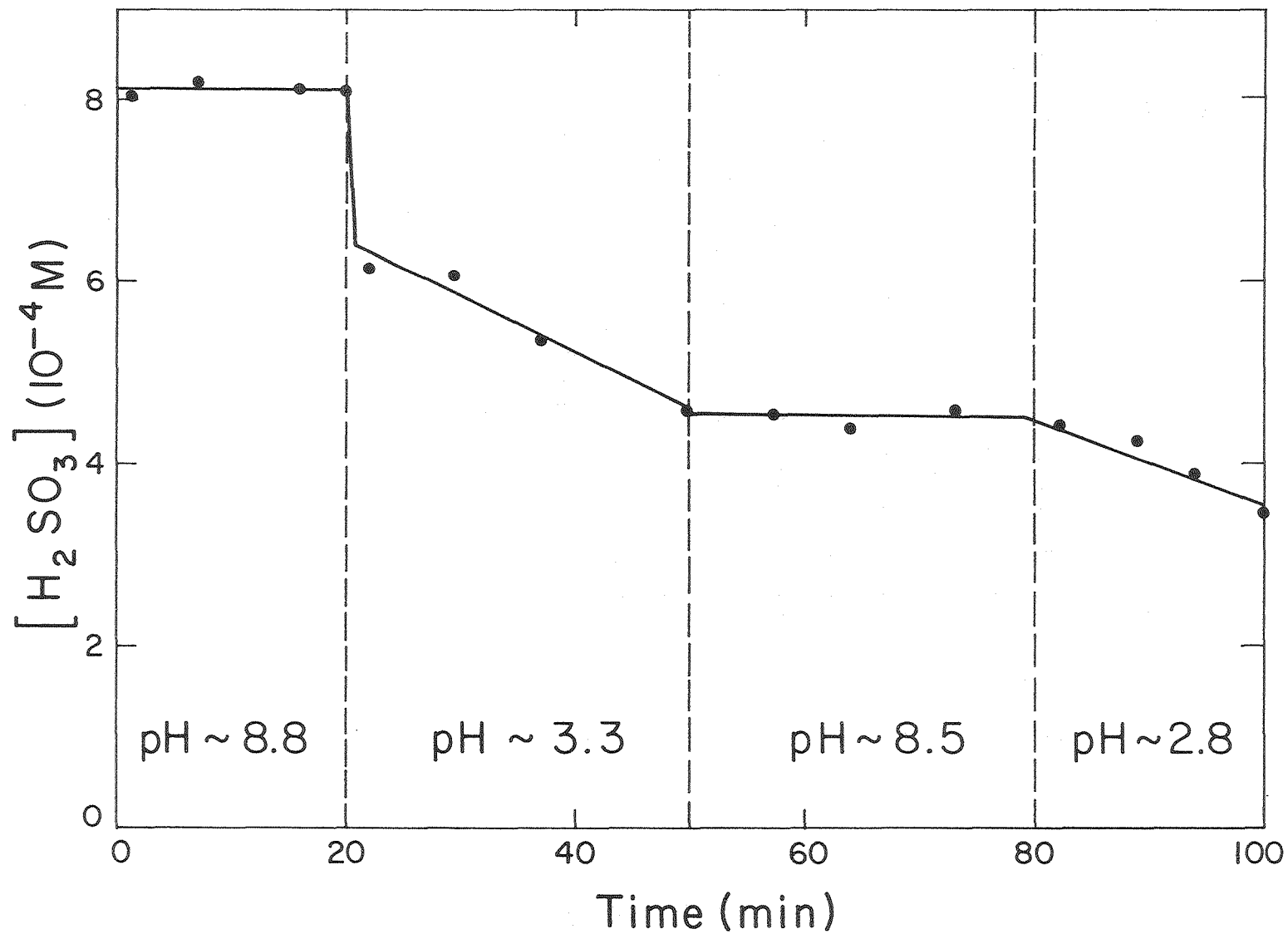
XBL 782-218

Figure 3.14  $H_2SO_3$  concentration versus time for a 1.6 g/l Nuchar C-190 suspension at various pH values.  $[H_2SO_3]_0 = 8.85 \times 10^{-4} M$ .

conditions. The pH range of these experiments more than covers the range normally seen for atmospheric water (rain, fog, etc.).

One of the most intriguing results of these studies is that no catalytic activity is seen above a pH of 7.6. Below pH = 7.6, the reaction rate is independent of the pH; but when the pH becomes greater than 7.6, no catalytic activity is observed. This behavior is the same for all three activated carbons. Figure 3.15 shows the behavior of the reaction as the pH is changed rapidly from acid to base by the addition of a few drops of concentrated NaOH or H<sub>2</sub>SO<sub>4</sub>. (Concentrations have been normalized to account for any dilution factors.) When the activated carbon, in this case Nuchar C-190, is placed into a mildly basic solution, no reaction occurs. When the solution is made mildly acidic, the reaction begins with the expected rate. Similar behavior is seen as the solution is changed back to basic and again to acidic. Although Fig. 3.15 shows this effect over a range of 5.5 pH units, a factor of 300,000 change in hydrogen-ion concentration, the abrupt drop in reaction rate occurs between pH 7.5 and 7.65, a factor of 1.4 change in hydrogen-ion concentration.

Attempts were made to buffer the pH of the solution using organic acid buffers. The presence of these buffers inhibited the reaction, most likely due to the adsorption of the buffer molecules onto the carbon surface. When water which was condensed from the atmosphere was used to prepare the reaction mixture, the oxidation proceeded as usual, even though the atmospheric water did have organic contaminants in it.



XBL7911-13281

Figure 3.15  $\text{H}_2\text{SO}_3$  concentration versus time as pH is quickly changed from basic to acidic.

### E. Other Surfaces

Alumina and ferric oxide were tried as catalysts, to test whether these high surface area materials could catalyze the reaction by their presence. No oxidation was observable due to the presence of these high-surface-area species. Leaching the activated carbon in concentrated sulfuric acid for 24 hours to remove trace metal impurities had no effect on the relative reactivity of that carbon.

To test if the reaction was being catalyzed by a species that could be washed off of the carbon surface, the activated carbon was washed and filtered. The filtrate was then prepared as the reaction mixture by the addition of S(IV) to it. No oxidation was observed in this solution. The reaction was also observed to be catalyzed by ground "spectroscopically pure" graphite as well as by the elemental carbon formed as a result of the addition of concentrated sulfuric acid to sugar.

## IV. DISCUSSION

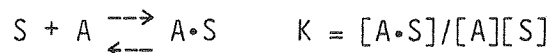
A. Mechanism

The experimental results yield the following reaction rate law for the catalytic oxidation of sulfur(IV) by activated carbon.

$$\frac{d[S(IV)]}{dt} = k[C_x] \frac{\gamma[O_2]}{1 + \gamma[O_2]} \frac{\alpha[S(IV)]^2}{1 + \beta[S(IV)] + \alpha[S(IV)]^2} \quad (IV.1)$$

The form of this equation is that of a reaction in which the reactant is adsorbed onto a surface.

The concentration of the adsorbed species is governed by the Langmuir isotherm [33]. The adsorption of reactant molecules A onto a surface S,



will cover a certain fraction,  $\theta$ , of the possible adsorption sites,

$$S^\circ = [A \cdot S] + [S]:$$

$$\theta = [A \cdot S]/S^\circ = K[A]/(1 + K[A]) \quad .$$

If the adsorbed species then reacts to form B;



the formation rate of B, assuming that the reverse of this reaction is negligible, is:

$$\begin{aligned}
 dB/dt &= k[A \cdot S] \\
 &= k[S]e \\
 &= k[S]K[A]/(1 + K[A]) \quad .
 \end{aligned}$$

The experimentally derived rate equation (IV-1) is already in this form for oxygen, and the S(IV) term can be broken into two factors;

$$\frac{\alpha[S(\text{IV})]^2}{1 + \beta[S(\text{IV})] + \alpha[S(\text{IV})]^2} = \frac{K_2[S(\text{IV})]}{1 + K_2[S(\text{IV})]} \times \frac{K_3[S(\text{IV})]}{1 + K_3[S(\text{IV})]}$$

$$\alpha = K_2K_3 \quad , \quad \beta = K_2 + K_3$$

The equation takes the form of the adsorption of one oxygen and two S(IV) molecules onto an activated carbon surface.

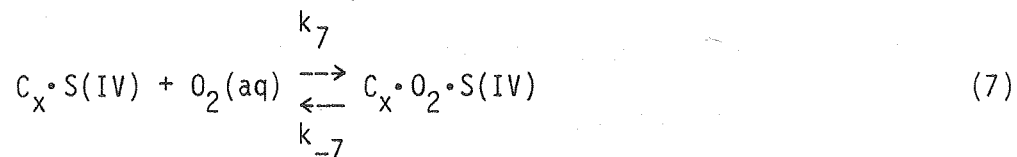
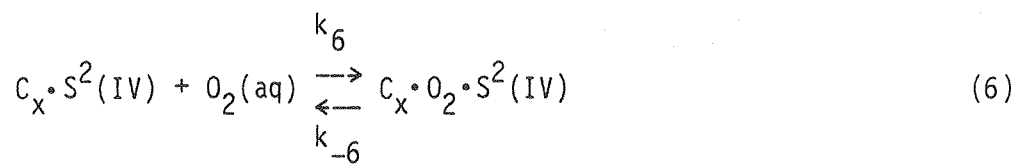
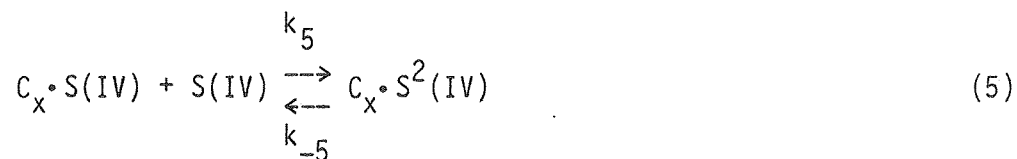
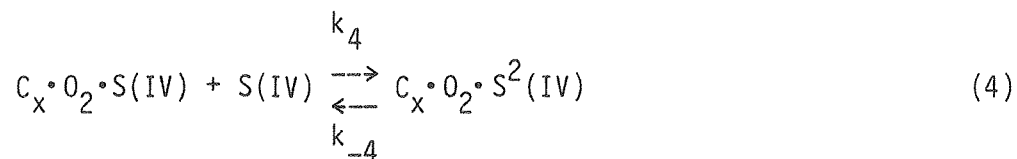
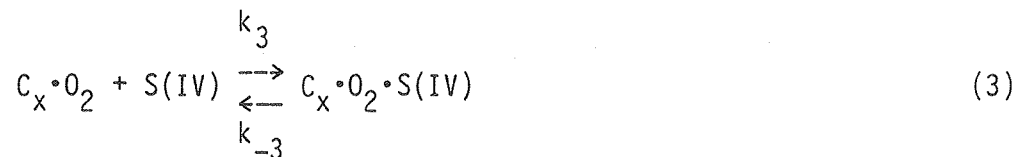
Symbolically, the net reaction for the oxidation of S(IV) is



The reduction of sulfate is not a thermodynamically favored reaction, and in these experiments does not occur. For this reason, the formation of sulfate will henceforth always be written as an irreversible reaction.

The following reactions are possible at the carbon surface.





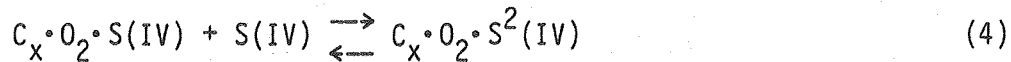
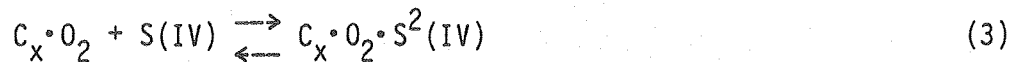
Steps 1 through 7 are assumed to be adsorptions on the surface, with the oxidation step occurring in reaction 8. Since the reaction occurs in water, the formation and desorption of the bisulfate or sulfate can be considered in one step.

The rate of production of the sulfate species is;

$$\text{Rate} = \frac{d[S(VI)]}{dt} = 2k_8[C_x \cdot O_2 \cdot S^2(IV)] \quad .$$

Since steps 1 and 2 are both initiation steps, it is simpler to derive a rate expression using each individually.

Assuming oxygen to be the first species adsorbed, the following four step reaction is arrived at.



The term,  $[C_x \cdot O_2 \cdot S^2(IV)]$ , can be solved for, by the Langmuir adsorption equation, as follows:

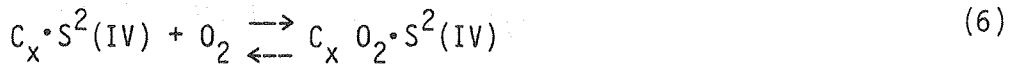
$$[C_x \cdot O_2 \cdot S^2(IV)] = \frac{K_4[S(IV)]}{1 + K_4[S(IV)]} [C_x \cdot O_2 \cdot S(IV)] \quad .$$

The same substitution to steps 3 and 1 can be applied, and the following is arrived at for the rate expression from these four steps:

$$\frac{d[S(VI)]}{dt} = 2k_8[C_x] \left( \frac{K_1[O_2]}{1 + K_1[O_2]} \right) \left( \frac{K_3[S(IV)]}{1 + K_3[S(IV)]} \right) \times \left( \frac{K_4[S(IV)]}{1 + K_4[S(IV)]} \right) \quad (IV.2)$$

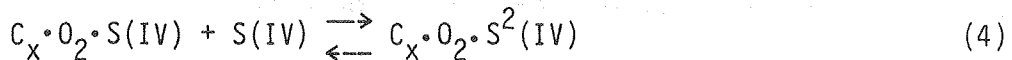
where  $K_1 = k_1/k_{-1}$ ,  $K_3 = k_3/k_{-3}$  and  $K_4 = k_4/k_{-4}$ .

Similar expressions can be arrived at for the following step sequences.



$$\frac{d[S(VI)]}{dt} = 2k_8[C_x] \left( \frac{K_2[S(IV)]}{1 + K_2[S(IV)]} \right) \left( \frac{K_5[S(IV)]}{1 + K_5[S(IV)]} \right) \times \left( \frac{K_6[O_2]}{1 + K_6[O_2]} \right) \quad (IV.3)$$

and



$$\frac{d[S(VI)]}{dt} = 2k_8[C_x] \left( \frac{K_2[S(IV)]}{1 + K_2[S(IV)]} \right) \left( \frac{K_7[O_2]}{1 + K_7[O_2]} \right) \times \left( \frac{K_4[S(IV)]}{1 + K_4[S(IV)]} \right) \quad (IV.4)$$

where  $K_2 = k_2/k_{-2}$ ,  $K_5 = k_5/k_{-5}$ ,  $K_6 = k_6/k_{-6}$  and  $K_7 = k_7/k_{-7}$ .

Combination of the rate equations (IV.2 - IV.4) gives an expression for the rate if all eight steps are possible.

$$\frac{d[S(VI)]}{dt} = 2k_8[C_x] \left\{ \left( \frac{K_2[S(IV)]}{1 + K_2[S(IV)]} \right) \left( \frac{K_5[S(IV)]}{1 + K_5[S(IV)]} \right) \left( \frac{K_6[O_2]}{1 + K_6[O_2]} \right) + \left( \frac{K_2[S(IV)]}{1 + K_2[S(IV)]} \right) \left( \frac{K_4[S(IV)]}{1 + K_4[S(IV)]} \right) \left( \frac{K_7[O_2]}{1 + K_7[O_2]} \right) + \left( \frac{K_1[O_2]}{1 + K_1[O_2]} \right) \left( \frac{K_3[S(IV)]}{1 + K_3[S(IV)]} \right) \left( \frac{K_4[S(IV)]}{1 + K_4[S(IV)]} \right) \right\} \quad (IV.5)$$

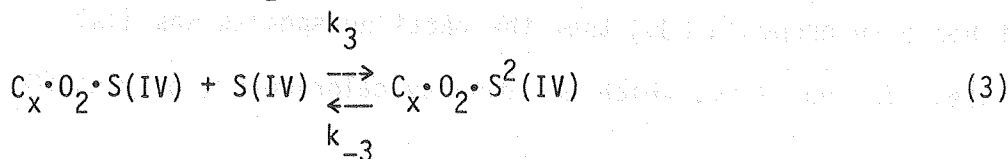
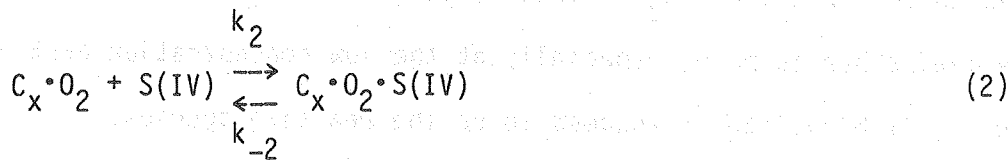
This identical equation is arrived at if the derivation is performed using all eight steps simultaneously. While equations (IV.2 - IV.4) all have the identical form as the experimental rate equation (IV.1), the combined rate equation (IV.5) cannot be reduced to the simple form of (IV.1), unless  $K_2 = K_3$ ,  $K_4 = K_5$  and  $K_1 = K_6 = K_7$ . Because equality of all the adsorption equilibrium constants is improbable, it is more probable that only one of these three four-step pathways is the dominant mechanism that is followed.

The experimental results seem to indicate that the adsorption of oxygen onto the activated carbon surface is the first step in the reaction. The experimentally observed activation energies are similar

to those seen for the chemisorption of oxygen onto activated carbons in the gas-phase [34]. Also, the behavior of the rapid initial oxidation indicates that it is the reaction of S(IV) with the  $C_x \cdot O_2$  complex which was formed prior to placing the carbon into the solution. When this preformed complex is removed by degassing the carbon prior to placing it in solution or equilibrating the carbon with the oxygen in solution prior to the addition of S(IV), the reaction proceeds according to the experimental rate expression without a rapid initial oxidation.

The behavior of the reaction when the pH is greater than 7.6 also indicates that oxygen adsorption is the initial step. Figure 3.15 shows that when the reaction is stopped (pH > 7.6), the S(IV) concentration is constant. No adsorption of S(IV) onto the carbon surface is apparent.

Assuming then that the first step in the reaction is the adsorption of dissolved oxygen, the following four steps (renumbered from above) will be the reaction mechanism:





with

$$\frac{d[S(IV)]}{dt} = 2k_4[C_x] \left( \frac{K_1[O_2]}{1 + K_1[O_2]} \right) \left( \frac{K_2[S(IV)]}{1 + K_2[S(IV)]} \right) \left( \frac{K_3[S(IV)]}{1 + K_3[S(IV)]} \right) \quad (IV.6)$$

where  $K_1 = k_1/k_{-1}$ ,  $K_2 = k_2/k_{-2}$  and  $K_3 = k_3/k_{-3}$ . Multiplication of the S(IV) terms yields the experimentally-obtained expression (IV.1),

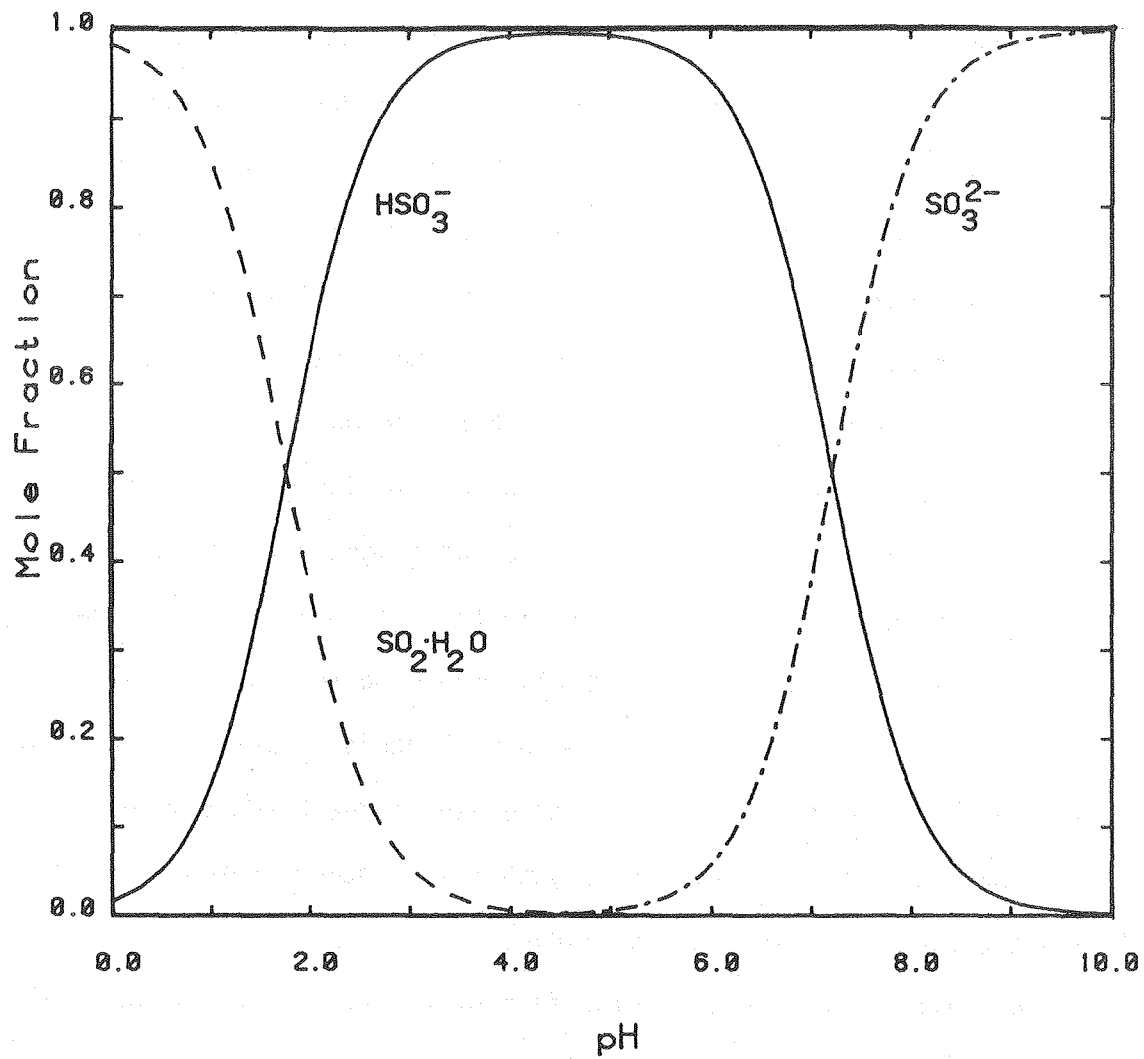
where  $K_2K_3 = \alpha$ ,  $K_2 + K_3 = \beta$  and  $K_1 = \gamma$ .

#### B. Effects of pH

The behavior of the reaction with respect to the pH of the solution seems to indicate that all three S(IV) species,  $SO_2 \cdot H_2O$ ,  $HSO_3^-$ , and  $SO_3^{2-}$ , react in a similar manner; hence the treatment of all species as one in the derivation of the rate law and mechanism.

Figure 4.1 shows the mole fraction of each of these species present as a function of pH. The range of conditions used in these studies covers pH values where each of the three S(IV) species can predominate. The rate of reaction is not affected by the differing mole fractions, and correction of the data for the concentration of just one of the species does not lead to any consistent rate law, if the reacting species is assumed to be  $SO_2 \cdot H_2O$  or  $SO_3^{2-}$ ; further, the fit to the rate law derived above is poor, especially at the low concentration part of the curve, if bisulfite is assumed to be the reacting species.

It has been proposed [35] that the reacting species was just bisulfite. In that work, which was done by calorimetry, only  $NaHSO_3$



XBL 8011-3931

Figure 4.1 Mole fraction of S(IV) species versus pH.

was used as a source for S(IV). No attempts were made to vary or control pH in those experiments. Because this work was done in a pH region where the mole fraction of bisulfite is greater than 0.95, the conclusion, while understandable, could not reasonably be made.

The abrupt disappearance of catalytic activity above pH 7.6 is not fully understood. The oxidation rates between pH 7 and 7.5 show that sulfite ion reacts equally as well as bisulfite. Also, the mole fraction of bisulfite just above pH 7.6 is not that small and oxidation should still be occurring, even if sulfite did not react.

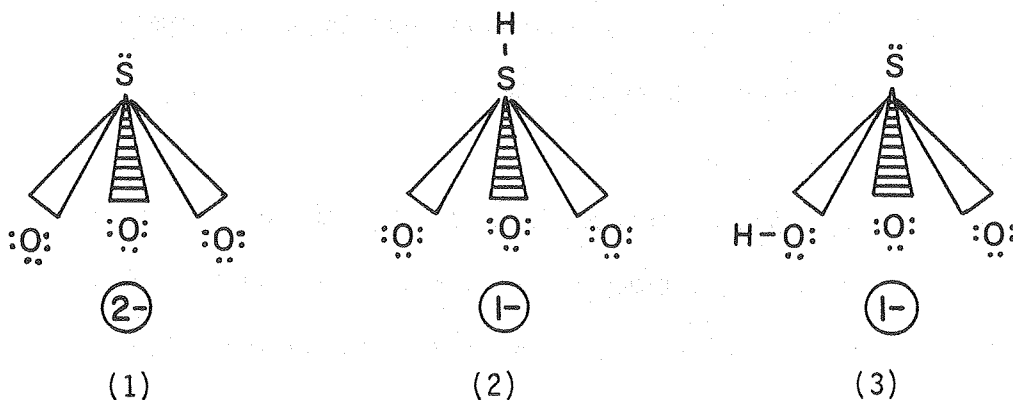
The data plotted in Fig. 3.15 do give some insight into this peculiar behavior. Apparently, the carbon-oxygen complex is modified in alkaline solution, in such a manner that it cannot react or desorb. This idea is supported by experiments, where, after the solution is made acidic for the first time, an initial rapid oxidation is observed. This rapid oxidation would not be observed if the  $C_x \cdot O_2$  complex had equilibrated with the dissolved oxygen (as is demonstrated at the second change from alkaline to acidic).

This effect was studied using each of the activated carbons. All three carbons exhibited the identical behavior with respect to this pH "cut off." The carbons themselves, however, are all different in affecting the pH of a solution when they are placed in that solution. Table II-1 shows the pH of degassed and deionized (pH = 7.00) water when each of the activated carbons is placed into the water at a concentration of 1 g/l. The activated carbons also act as weak but continuous buffers in the pH range 1 to 10.

From these results, it can be assumed that a specific type of site on the activated carbon surface is the catalytically active site. This allows for the identical behavior of the different carbons with the pH "cut off" as well as the different coefficients for the experimental rate law. The catalytic activity of a given surface will be dependent on the method of activation and the other "history" of that carbon. For a specific activated carbon (or soot), the concentration of active sites present will be proportional to the effective (or interfacial) surface area. This proportionality differs, though, from carbon to carbon.

A possible physico-chemical explanation of the reaction is that the active carbon-oxygen complex is a Lewis acid. This would account for the adsorption and reaction of the S(IV) ions, which are Lewis bases.

The structure of the sulfite ion is known to be pyramidal in the crystalline form [36]. A possible electron-dot structure of the ion in solution could be that of structure (1), with the oxygens at the base of the pyramid. The bisulfite ion is known



to have two structures- (2) and (3), which are in equilibrium with each other. Both of these, again, have the oxygens at the base of the pyramid. The bisulfite ion with the hydrogen on an oxygen and the sulfite ion both have lone electron pairs on the sulfur which can act as a Lewis base. These could then combine with the carbon-oxygen Lewis acid to form the reaction complex.

The apparent reaction of hydrated  $\text{SO}_2$  on the activated carbon would seem to contradict the preceding explanation.  $\text{SO}_2$  is normally considered a Lewis acid and reacts as such in most cases. There is a lone electron pair on the sulfur however, and when the molecule is hydrated, it could be sufficiently electronegative to act as a Lewis base. It is also possible that the hydrated  $\text{SO}_2$  is not a reactant. A change of the total S(IV) concentration to just that of bisulfite for the experiments done at pH below 2 does not change the fit of the rate versus concentration curve very much. Experiments that would show clearly whether or not the hydrated sulfur dioxide reacts were not possible to perform with the analytic methods available. The concentration of  $\text{SO}_2$  and the acidity of solution that these experiments would require also removes them from any significance to the atmospheric pollution studies.

The preceding explanation could account for the pH "cut-off" effect if the carbon-oxygen-complex Lewis acid is assumed to have a  $\text{pK}_a$  of 7.6. A gradual decrease in reaction rate, however, should be seen as pH increases if this were the case. The change in magnitude of the catalyzed-to-uncatalyzed reaction rates is ~100 fold. At a factor of 1.4 change in hydrogen-ion concentration, the hydrogen-ion

dependence of the reaction would need to be approximately thirteenth order. A dependence of this magnitude would be observed at the lower pH values as well, if it were the sulfurous acid oxidation reaction that had the dependence. One possibility is that a competing reaction, highly dependent on hydrogen-ion concentration, uses the carbon-oxygen complex. This reaction would have a rate which becomes significant with respect to the S(IV) oxidation rate above pH 7.6, and is negligible below pH 7.6.

This possible competing reaction is most likely an equilibrium (or a series of equilibria) type reaction where the carbon-oxygen complex reacts to form a catalytically inactive complex. As hydrogen-ion concentration is increased, so that the pH becomes less than 7.6 the equilibria shift back towards the active carbon-oxygen complex. This explanation also accounts for the observed behavior that, when activated carbon is placed in suspension, the oxygen adsorbed on the surface does not equilibrate with the solution.

Though the pH (below 7.6) of the solution does not affect the reaction rate, it does play an important role when this mechanism is extrapolated to atmospheric conditions. The kinetic studies were all done starting with S(IV) species in solution. For this reaction to occur in a polluted environment, it is necessary to get the  $\text{SO}_2$  into a droplet-solution. It is the solubility of  $\text{SO}_2$  that is a function of pH, due to the diprotic nature of  $\text{SO}_2 \cdot \text{H}_2\text{O}$ . At equilibrium, the total S(IV) concentration is given by the equation

$$[S(IV)_{aq}] = C_{SO_2} P_{SO_2} ([H^+]^2 + K_1[H^+] + K_1K_2)/[H^+]^2$$

where  $C_{SO_2}$  = Henry's Law constant for  $SO_2$ , 1.30 M/atm at 25°C [37],  
 $P_{SO_2}$  = pressure of  $SO_2$  in atmospheres, and  $K_1$  and  $K_2$  are the  
 first and second acid dissociation constants for sulfurous acid;  
 $K_1 = 1.7 \times 10^{-2}$ ,  $K_2 = 5.5 \times 10^{-8}$  [38]. The pH of a droplet  
 will not be a fixed, buffered quantity, but is a function of all the  
 species in solution, including the sulfur dioxide, carbon dioxide and  
 subsequently formed sulfate.

### C. Confirmation of Results

Since the initial publication of the early results of these  
 experiments [39,40], the catalytic oxidation of S(IV) on activated  
 carbons in the presence of water has been seen to occur by other  
 researchers [35,41]. These works support the importance of liquid  
 water in enhancing the oxidation rate. Neither work, though, does any  
 systematic kinetic studies; they fall more into the realm of  
 qualitative, rather than quantitative studies.

Fog chamber studies done at Lawrence Berkeley Laboratory's  
 Atmospheric Aerosol Research Group [42] serve to confirm strongly this  
 reaction. Sulfate formation rates in fog droplets, created by  
 nebulization of an activated carbon slurry, were measured. These  
 rates, when normalized to the carbon concentration present, show a  
 similar behavior with respect to  $SO_2$  concentration, as does the rate  
 in solution versus total S(IV) concentration in solution. The fog  
 chamber studies are a major step towards understanding the applications  
 of this reaction in "real world" terms.

## V. SUMMARY AND CONCLUSIONS

The goal of this work was to acquire a better understanding of the role that combustion-produced-soot particles play in the oxidation of sulfur dioxide to sulfate in a polluted environment. For this goal to be achieved, it has been necessary to study first the catalytic nature of activated carbon in solutions containing sulfur(IV) species. These studies were performed by mixing solutions of S(IV) with various activated carbons and soots, and following the decrease in S(IV) concentration and concurrent increase in sulfate concentration.

This research has shown that activated carbons in aqueous suspension are effective catalysts for the oxidation of the S(IV) species. The behavior of the reaction can be summarized as follows:

1. The reaction rate is independent of pH ( $\text{pH} < 7.6$ ), and therefore  $\text{SO}_2 \cdot \text{H}_2\text{O}$ ,  $\text{HSO}_3^-$  and  $\text{SO}_3^{2-}$  are indistinguishable (within the limits of this research) in terms of oxidation on the carbon surfaces.
2. The reaction is first order with respect to the concentration of carbon particles.
3. The reaction rate has a complex dependence on the concentration of S(IV), ranging between a second and zeroth order reaction as the S(IV) concentration increases (Langmuir adsorption).
4. The reaction rate has a complex dependence on the concentration of dissolved  $\text{O}_2$ , ranging between a first and zeroth order reaction as the  $\text{O}_2$  concentration increases (Langmuir adsorption).
5. The activation energy of the reaction is  $\sim 8.5$  kcal/mole, with each different carbon having slightly differing values.

A possible four step reaction mechanism, consistent with all experimentally observed results, has been proposed. The mechanism consists of the step-wise adsorption of the reactants, oxygen and sulfur(IV), onto the carbon surface with a subsequent oxidation to sulfate, which desorbs from the surface, regenerating the catalytically active site.

As with most scientific research, new questions have arisen from these results. The study of the properties of the catalytically active site is one that this author feels is of significant importance. An understanding of these sites (how they are formed, how to measure them, and what their behavior with pH is) will help extend this research into the field of air pollution knowledge and control.

With the growing shift in the United States back to the use of coal as a major energy source, a potential exists for a dramatic increase in sulfur emissions and, consequently, in the formation of acid rain. This research will aid in the understanding of the formation of acid rain because the chemical reaction studied in this thesis can be a major contributor to the formation of atmospheric sulfates. It is this author's hope that, from this work and future research, the problems of air pollution will be completely understood and that proper control strategies, which preserve and protect our environment, will be introduced.

## ACKNOWLEDGEMENTS

I wish to thank, first and foremost, Mr. Richard Poppe, chemistry teacher at Terra Linda High School, San Rafael, CA, who first piqued my curiosity in the study of chemistry.

I wish to thank my research advisor, Prof. Samuel Markowitz, Dr. Tihomir Novakov and all the members of the Lawrence Berkeley Laboratory's Atmospheric Aerosol Research Group for all their help, encouragement and ideas during my graduate studies.

My love and heartfelt thanks go to my wife, Jackie, for the love and support given to me, and to my parents and sister for everything they've done for me over the years. And to my parents I would like to say, "Yes! I am finished now."

The support of the Assistant Secretary for the Environment, Office of Health and Environmental Research, Pollutant Characterization and Safety Research, Division of the U.S. Department of Energy (Contract No. W-7405-ENG-48) and the National Science Foundation is gratefully acknowledged.

## APPENDIX A-1

## Sample titration and turbidity data

0.31615g Nuchar C-190  $[I_3^-] = 5.10 \times 10^{-4} \text{ M}$   $[S_2O_3^{2-}] = 1.00 \times 10^{-3} \text{ M}$   
 initial volume = 200.0 ml  $[S(IV)]_0 = 8.85 \times 10^{-4} \text{ M}$

time min	V <sub>soln</sub> ml	V <sub>I<sub>3</sub><sup>-</sup></sub> ml	V <sub>S<sub>2</sub>O<sub>3</sub><sup>2-</sup></sub> ml	abs (A)	[S(IV)] 10 <sup>-4</sup> M	[SO <sub>4</sub> <sup>2-</sup> ] 10 <sup>-4</sup> M
0				0.005	8.85	0.0
1.0	10.0	15.0	2.50	0.060	6.40	1.49
5.0	10.0	15.0	3.10	-	6.10	-
7.0	-	-	-	0.080	-	2.07
10.0	10.0	15.0	4.20	-	5.55	-
15.0	10.0	10.0	0.70	0.139	4.75	3.77
20.0	10.0	10.0	1.40	-	4.40	-
25.0	10.0	10.0	2.40	0.180	3.90	4.95
30.0	10.0	10.0	4.00	-	3.10	-
33.0	-	-	-	0.20	-	5.53
35.5	10.0	10.0	4.70	-	2.75	-
40.0	10.0	10.0	4.80	-	2.70	-
42.0	-	-	-	0.231	-	6.42
45.0	10.0	10.0	6.50	-	1.85	-
48.0	-	-	-	0.262	-	7.32
50.0	10.0	5.0	2.20	-	1.45	-

relative standard deviation of concentrations:  $\pm 2.0$  percent.

## Sulfate calibration

$\mu\text{g/ml}$ Sulfate	absorbance (A) $\lambda = 500\text{nm}$
0.0	0.0
20.0	0.060
40.0	0.178
60.0	0.243
80.0	0.311
100.	0.342

$$\mu\text{g/ml SO} = 2.77 \times 10^2 \text{ A} - 2.34$$

$$r^2 = 0.974$$

## APPENDIX A-2

## Sample IC data

11.76mg Aktivkohle initial volume = 900.8ml

(900.0 ml H<sub>2</sub>O + 0.8ml 1000µg/ml SO<sub>3</sub><sup>2-</sup>)

time min	V <sub>inj</sub> ml	sulfite		sulfate		[S(IV)]	[SO <sub>4</sub> <sup>2-</sup> ]
		peak ht cm	full sc µmho	peak ht cm	full sc µmho	10 <sup>-6</sup> M	10 <sup>-6</sup> M
1.5	1.0	12.9	1.0	1.6	1.0	8.33	1.98
22.0	1.0	11.7	1.0	2.9	1.0	7.67	2.25
41.0	1.0	10.5	1.0	5.3	1.0	7.02	2.75
61.0	2.0	18.0	1.0	13.2	1.0	5.55	2.20
82.0	2.0	15.3	1.0	17.1	1.0	4.81	2.61
102.5	2.0	12.9	1.0	2.1	10.0	4.16	3.02
123.0	2.0	11.1	1.0	2.5	10.0	3.67	3.44
146.0	2.5	10.4	1.0	3.3	10.0	2.79	3.42
166.0	2.5	8.7	1.0	3.7	10.0	2.42	3.76
187.0	2.5	6.6	1.0	4.1	10.0	1.96	4.09
209.0	2.0	13.2	0.3	11.7	3.0	1.74	4.50
230.0	2.0	9.2	0.3	12.0	3.0	1.41	4.59
251.5	4.0	13.8	0.3	off scale		0.892	-
273.0	4.0	8.9	0.3	"		0.692	-
296.0	5.0	6.9	0.3	"		0.489	-
322.0	5.0	4.0	0.3	"		0.394	-

relative standard deviation of concentrations: ±2.0 percent

## Calibrations

sulfite µg	pk ht cm	full sc µmho	sulfate µg	pk ht cm	full sc µmho
0.50	3.0	3.0	0.30	3.0	3.0
0.75	15.0	1.0	0.45	12.0	1.0
1.00	20.5	1.0	0.60	2.25	10.0

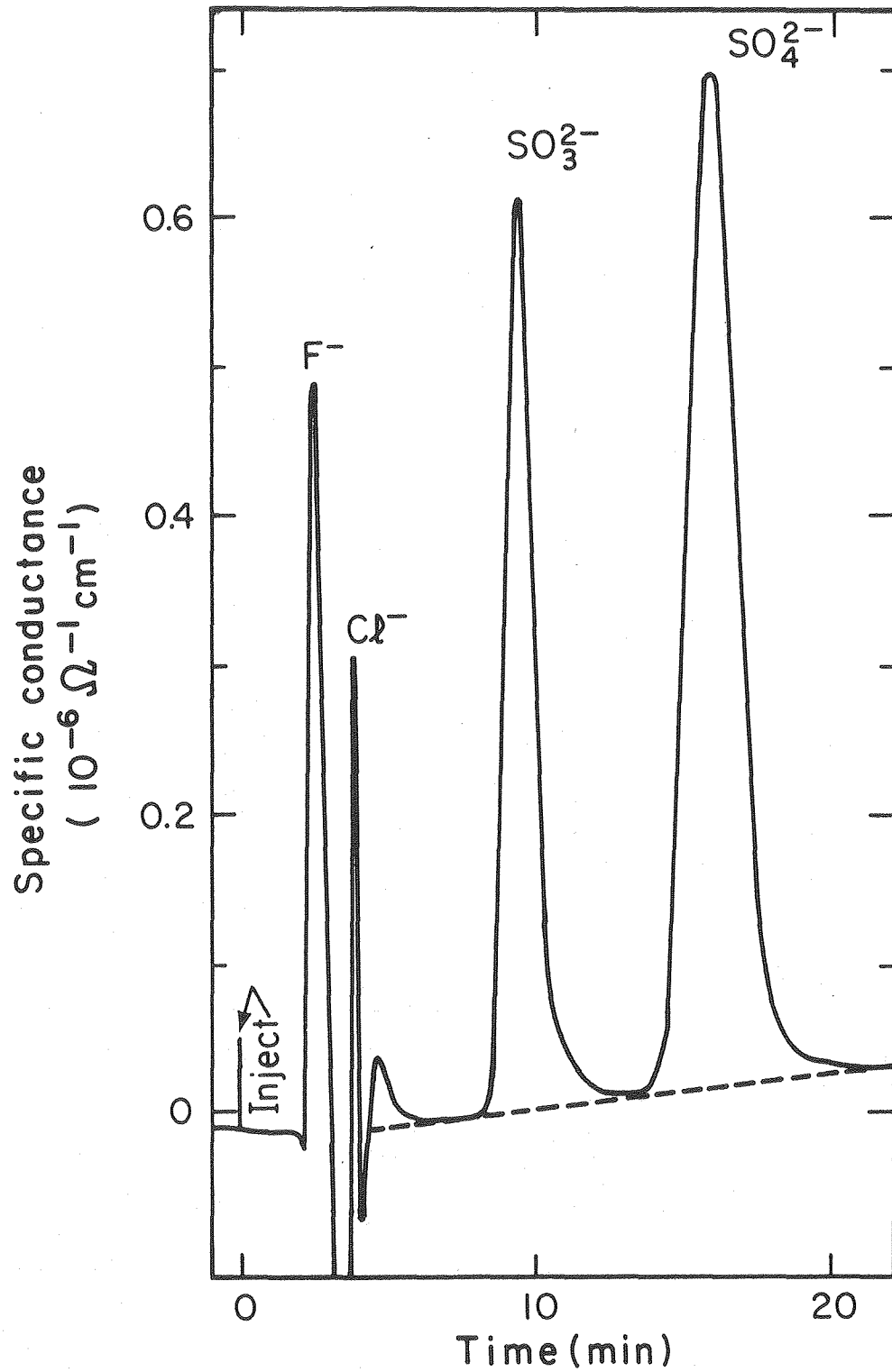
$$\mu\text{g}(\text{SO}_3^{2-}) = 0.1055 + 1.104\mu\text{mho}$$

$$r^2 = 0.999$$

$$\mu\text{g}(\text{SO}_4^{2-}) = 0.1578 + 0.5118\mu\text{mho}$$

$$r^2 = 0.907$$

full sc = full scale on chart recorder



XBL 8010-2276

Figure A2.1 Sample ion chromatogram.

## APPENDIX B. Error Analysis and Computational Methods

Error analysis of results from these experiments falls into two categories, experimental uncertainties due to the analytical techniques used and the statistical uncertainties that arise from the many calculations that were performed on the experimental data.

The experimental uncertainties or tolerances are summarized in the following tables.

Table B-1  
Titration and Turbidity Tolerances

$[S_2O_5^{2-}]$	0.1% <sup>†</sup>
$[I_3^-]$	0.5% <sup>†</sup>
time	0.25 min *
volume of soln or $I_3^-$	0.1 ml **
volume of $S_2O_5^{2-}$	0.05 ml **
absorbance	0.002 abs units*
$SO_4^{2-}$ stds	0.1 $\mu\text{g/ml}$ <sup>†</sup>

Table B-2  
Ion Chromatography Tolerances

time	0.5 min *
inject volume	0.1 ml *
peak height	0.1 cm *
standards	1.0% <sup>†</sup>

- † calculated standard deviation  
\* estimated standard deviation  
\*\* instrumental standard deviation

The values of pH were measured to  $\pm 0.05$  pH units, temperature to  $\pm 0.5^\circ\text{C}$  and oxygen concentration to within 5 percent. The mass of the catalyst used was measured to  $\pm 0.1$  mg and the initial volume of reaction mixture to 0.5 mL.

The method of root-mean-square can be used to calculate the uncertainties in the values for the concentrations of S(IV) and sulfate for each experimental point. These calculations yield values for the standard deviations from 1.5 percent to as much as 5.0 percent, with the majority of values around 2.0 percent.

Calculation of the S(IV) concentration from the titration data was done by the formula

$$[\text{S(IV)}] = \frac{V_I M_I - (V_T M_T / 2)}{V_S}$$

where  $V_S$ ,  $V_I$  and  $V_T$  are, respectively, the volumes of reaction solution, triiodide and thiosulfate titrant used in the titration and  $M_I$  and  $M_T$  are the molar concentrations of the triiodide and thiosulfate. Sulfate concentrations from the turbidimetric method are calculated by the Beer's Law equation, the coefficients calculated by a least-squares fit of the data obtained with standard solutions.

Concentration values for the ion chromatography experiments are obtained from least-squares fits of standard solutions. Full scale measurements on the chart recorder are 25.4 cm. A total amount of ionic species is determined and then divided by the volume injected to determine concentration.

The least-squares calculations for the linear and polynomial fits were done using the FORTRAN language subroutines, LINFIT and POLFIT, as developed and described by Bevington [43]. The calculations were performed on a DEC LSI-11 microcomputer, with the RT-11, version 3B operating system. A FORTRAN master program was written to calculate S(IV) and sulfate concentrations from the ion chromatography experiments' raw data, and then to calculate from the time-concentration data of either the titration or IC experiments, three point average rates of reaction to be used in the polynomial least-squares fits.

Linear least-squares were calculated by solving [44] the simultaneous equations:

$$\begin{aligned}\sum y_i / \sigma_i^2 &= a \sum 1 / \sigma_i^2 + b \sum x_i / \sigma_i^2 \\ \sum x_i y_i / \sigma_i^2 &= a \sum x_i / \sigma_i^2 + b \sum x_i^2 / \sigma_i^2\end{aligned}$$

the solutions of which are:

$$a = (\sum x_i^2 / \sigma_i^2 \sum y_i / \sigma_i^2 - \sum x_i / \sigma_i^2 \sum x_i y_i / \sigma_i^2) / \Delta$$

$$b = (\sum 1 / \sigma_i^2 \sum x_i y_i / \sigma_i^2 - \sum x_i / \sigma_i^2 \sum y_i / \sigma_i^2) / \Delta$$

$$\Delta = \sum 1 / \sigma_i^2 \sum x_i^2 / \sigma_i^2 - (\sum x_i / \sigma_i^2)^2$$

Polynomial least-squares are calculated by solving the simultaneous equations [45] which are just the extrapolation of the linear equations. These equations are somewhat different than normally seen, as the fits are weighted by the standard deviations ( $\sigma_i^2$ ) of the dependent variables ( $y_i$ ). Standard deviations of the coefficients a and b can be solved for as well. They are:

$$\sigma_a^2 = 1/\Delta \sum x_i^2 / \sigma_i^2 \quad \text{and} \quad \sigma_b^2 = 1/\Delta \sum 1/\sigma_i^2 \quad ,$$

where  $\Delta$  is as before. The computer subroutines LINFIT and POLFIT compute the values of the coefficients as well as their standard deviations.

Using these equations, the reaction rate versus S(IV) concentration data were calculated by taking every three data points from an experimental run. If, for example, a run had seven data points, five reaction rates versus concentration points would be calculated, from points 1-2-3, 2-3-4, etc. The rates were calculated using the linear least-squares, with  $x = \text{time}$ ,  $y = [S(\text{IV})]$  and  $\sigma = 0.02y$ . The rate is then the slope of the calculated line, or as written above, the coefficient  $b$ . The average concentration is calculated from the three points and it, along with the calculated rate and its standard deviation,  $\sigma_b$ , is used as one of the points for the polynomial fit.

The equation which fits the rate versus S(IV) concentration data:

$$y = k\alpha x^2 / (1 + \beta x + \alpha x^2)$$

with  $y = \text{rate}$  and  $x = [S(\text{IV})]$ , can be converted to a second order polynomial by inverting the equation:

$$v = a + bu + cu^2$$

with  $v = 1/y$ ,  $u = 1/x$ ,  $a = 1/k$ ,  $b = \beta/k\alpha$  and  $c = 1/k\alpha$ . A similar inversion technique was used for fitting the rate versus oxygen concentration data to the equation:

$$\text{rate} = k\gamma[O_2]/(1 + \gamma[O_2])$$

In this case, the inverted equation is a linear function.

One source of error that could not be handled statistically was the non-homogeneity of the catalytic site concentration on the activated carbons used. Reproducible rate results were generally obtained from similar experiments; the lack of homogeneity in the carbons used, however, led to results that varied by 10-50 percent. Experiments in which relatively large amounts of carbon were used showed much less variations than did those in which smaller quantities were present. These variations are artifacts of the manufacture of the activated carbons. The Aktivkohle caused the least variation in the rates and the Nuchar C-190 the most.

## APPENDIX C.

Abstract from:

Kinetics and Mechanism for the Catalytic Oxidation of  
Sulfur Dioxide on Carbon in Aqueous Suspensions\*

R. Brodzinsky, S. G. Chang, S. S. Markowitz, and T. Novakov

Combustion-produced soot (carbonaceous) particles have been found to be efficient catalysts for  $\text{SO}_2$  oxidation, especially in the presence of liquid water. A kinetic study of the catalytic oxidation of  $\text{SO}_2$  on carbon particles suspended in solution has been carried out. The reaction was found to be first order with respect to the concentration of carbon particles, 0.69th order with respect to dissolved oxygen, between zero and second order with respect to  $\text{S(IV)}$  concentrations, and independent of the pH. Temperature studies were carried out, and an activation energy for this reaction was determined. A four-step mechanism is proposed for this carbon-catalyzed oxidation reduction.

\* J. Phys. Chem. 1980, 84, 3354-3358.

## References and Footnotes

1. W. W. Kellogg, R. D. Cadle, E. R. Allen, A. L. Lazrus and E. A. Matell, *Science*, 175, 587 (1972).
2. D. L. Coffin and H. E. Stokmayer, "Biological Effects of Air Pollution" in "Air Pollution, 3rd Edition," A. C. Stern, Ed., Vol. II, Academic Press, New York, 1977, pp 289-305.
3. S. West, *Science News*, 117, 76 (1980).
4. D. J. O'Brien, F. B. Birkner, *Envir. Sci. Tech.*, 11, 1114 (1977).
5. C. Junge, T. G. Ryan, *Quart. J. Roy. Met. Soc.*, 84, 46 (1958).
6. W. D. Scott, P. V. Hobbs, *J. Atm. Sci.*, 24, 54 (1967).
7. J. M. Miller, R. G. dePena, *J. Geophys. Res.*, 77, 5905 (1972).
8. S. Beilke, D. Lamb and J. Muller, *Atm. Env.*, 9, 1083 (1975).
9. H. F. Johnstone, R. R. Coughanowar, *Ind. Eng. Chem.*, 50, 972 (1958).
10. M. J. Matteson, *et al.*, *Ind. Eng. Chem.*, 8, 667 (1969).
11. J. Freiberg, *Atm. Env.*, 9, 661 (1975).
12. J. Freiberg, *Envir. Sci. Tech.*, 8, 731 (1974).
13. J. Freiberg, *Atm. Env.*, 10, 121 (1976).
14. R. E. Erickson, L. M. Yates, R. L. Clark and D. McEwen, *Atm. Env.*, 11, 813 (1977).
15. D. Moller, *Atm. Env.*, 14, 1067 (1980).
16. H. Rosen, A.D.A. Hansen, R. L. Dod and T. Novakov, *Science*, 208, 741 (1980).
17. U. Hoffman, D. Wilm, *Z. Elektrochem. Angew. Physik. Chem.*, 42, 504 (1936).

18. M. Hartman, R. W. Coughlin, Chem. Eng. Sci., 27, 867 (1972).
19. B. R. Appel, E. L. Kothny, E. M. Hoffer and J. J. Wesolowski, "Sulfate and Nitrate Data from...", in "Character and Origins of Smog Aerosols," G. Hidey, et. al., Eds., J. Wiley and Sons, New York, 1980, pp 315-335.
20. A.D.A. Hansen, Lawrence Berkeley Laboratory, private comm., (1980).
21. T. Novakov, Lawrence Berkeley Laboratory, private comm., (1980).
22. T. Novakov, S. G. Chang and A. B. Harker, Science, 186, 259 (1974).
23. T. Novakov, S. G. Chang, AIChE Sym. Ser., 72, 255 (1975).
24. Estimates of carbon concentrations in fog droplets were calculated by taking typical ambient carbon and liquid water concentrations/ $m^3$  and assuming 10-50 percent of the carbon was in solution. Droplets do not evaporate to dryness as organics can act as surfactants, inhibiting evaporation.
25. The coal burner used was built by Frank Robbin of Lawrence Berkeley Laboratory.
26. While the word 'Aktivkohle' is simply the German word for activated carbon, it will be used within the body of this work to mean the specific activated carbon manufactured by E. Merck.
27. D. Peters, J. Hayes and G. Hieftje, "Chemical Separations and Measurements," W. B. Saunders, Philadelphia, 1974. For a more detailed description of iodometric techniques see pp 322-338.
28. ibid, pp 231-233.
29. L. J. Holcombe, E. E. Ellsworth, B. F. Jones and F. B. Meserole, Radian Corp. Report No. 320-403-05, 1978.

30. E. E. Ellsworth, Radian Corp., private comm., (1979).
31. J. Menear, Dionex Corp., private comm., (1979).
32. S. W. Benson, "The Foundations of Chemical Kinetics," McGraw-Hill, New York, 1960, pg 67.
33. ibid, pg 624.
34. B. R. Puri, D. D. Singh and K. C. Sehgal, J. Indian Chem. Soc., 48, 513 (1971).
35. D. J. Eatough, W. P. Green and L. D. Hansen, in "Proceedings of the Conference on Carbonaceous Particles in the Atmosphere," T. Novakov, Ed., Lawrence Berkeley Laboratory Report LBL-9037, p. 131 (1979).
36. F. A. Cotton and G. Wilkinson, "Advanced Inorganic Chemistry," 3rd ed., J. Wiley and Sons, New York, 1972, pg. 448.
37. A. J. Gordon, R. A. Ford, "The Chemists' Companion," John Wiley and Sons, New York, 1972, pg. 39.
38. D. Peters, et. al., see Ref. 27, pg. A.9.
39. S. G. Chang, R. Brodzinsky, S. S. Markowitz and T. Novakov, Atmospheric Aerosol Research Annual Report 1976-7, Lawrence Berkeley Laboratory Report LBL-6819, 1977, pp 42-56.
40. S. G. Chang, R. Brodzinsky, R. Toossi, S. S. Markowitz, T. Novakov, in "Proceedings of the Conference on Carbonaceous Particles in the Atmosphere," T. Novakov, Ed., Lawrence Berkeley Laboratory Report LBL-9037, pg. 122 (1979).
41. W. R. Cofer, D. R. Schryer and R. S. Rogowski, *Atm. Env.*, 14, 571 (1980).

42. W. H. Benner, R. Brodzinsky and T. Novakov, "Fog Chamber Studies of Soot-Catalyzed  $\text{SO}_2$  Oxidation," presented at Department of Energy Meeting, Harpers Ferry, West Virginia, May, 1980.
43. P. R. Bevington, "Data Reduction and Error Analysis for the Physical Sciences," McGraw-Hill, New York, 1969.
44. ibid. Detailed derivations of these equations are given in Chapter 6, pp. 92-117.
45. ibid., Chapter 8, pp. 134-163.